6 THE MATHEMATICAL THEORY OF PLASTICITY

THE mathematical theory of plasticity provides a general framework for the continuum constitutive description of the behaviour of an important class of materials. Basically, the theory of plasticity is concerned with solids that, after being subjected to a loading programme, may sustain permanent (or *plastic*) deformations when completely unloaded. In particular, this theory is restricted to the description of materials (and conditions) for which the permanent deformations do *not* depend on the rate of application of loads and is often referred to as *rate-independent* plasticity. Materials whose behaviour can be adequately described by the theory of plasticity are called *plastic* (or *rate-independent plastic*) materials. A large number of engineering materials, such as metals, concrete, rocks, clays and soils in general, may be modelled as plastic under a wide range of circumstances of practical interest. The origins of the theory of plasticity can be traced back to the middle of the nineteenth century and, following the substantial development that took place, particularly in the first half of the twentieth century, this theory is today established on sound mathematical foundations and is regarded as one of the most successful phenomenological constitutive models of solid materials.

The present chapter reviews the mathematical theory of plasticity. The theory presented here is restricted to infinitesimal deformations and provides the basis for the numerical simulation of the behaviour of elastoplastic solids to be discussed in Chapter 7. We remark that only the most important concepts and mathematical expressions are reviewed. Attention is focused on the description of mathematical models of elastoplastic materials and, in particular, issues such as limit analysis and slip-line field theory are not addressed. For a more comprehensive treatment of the theory of plasticity, the reader is referred to Hill (1950), Prager (1959), Lubliner (1990) and Jirásek and Bažant (2002). A more mathematically oriented approach to the subject is presented by Halphen and Nguyen (1975), Duvaut and Lions (1976), Matthies (1979), Suquet (1981) and Han and Reddy (1999).

This chapter is organised as follows. In Section 6.1, aspects of the phenomenological behaviour of materials classed as plastic are discussed and the main properties are pointed out in the analysis of a simple uniaxial tension experiment. The discussion is followed, in Section 6.2, by the formulation of a mathematical model of the uniaxial experiment. The uniaxial model, though simple, embodies all the essential concepts of the mathematical theory of plasticity and provides the foundation for the general multidimensional model established in Section 6.3. The remainder of the chapter focuses on the detailed description of the plasticity models most commonly used in engineering analysis: the models of Tresca, von Mises, Mohr–Coulomb and Drucker–Prager. The corresponding yield criteria are

Computational Methods for Plasticity: Theory and Applications EA de Souza Neto, D Perić and DRJ Owen

described in Section 6.4. Plastic flow rules and hardening laws are addressed, respectively, in Sections 6.5 and 6.6.

6.1. Phenomenological aspects

In spite of their qualitatively distinct mechanical responses, materials as contrasting as metals and soils share some important features of their phenomenological behaviour that make them amenable to modelling by means of the theory of plasticity. To illustrate such common features, a uniaxial tension experiment with a metallic bar is discussed in what follows.

Typically, uniaxial tension tests with ductile metals produce stress–strain curves of the type shown in Figure 6.1. In the schematic diagram of Figure 6.1, where the axial stress, σ, is plotted against the axial strain, ε, a load programme has been considered in which the bar is initially subjected to a monotonic increase in axial stress from zero to a prescribed value, σ_0. The bar is then unloaded back to an unstressed state and subsequently reloaded to a higher stress level σ_1. The stress–strain curve follows the path $O_0Y_0Z_0O_1Y_1Z_1$ shown. In this path, the initial line segment O_0Y_0 is virtually straight and, if the bar is unloaded from point Y_0 (or before it is reached), it returns to the original unstressed state O_0. Thus, in segment O_0Y_0 the behaviour of the material is regarded as *linear elastic*. Beyond Y_0, the slope of the stress–strain curve changes dramatically and if the stress (or strain) loading is reversed at, say, point Z_0, the bar returns to an unstressed state via path Z_0O_1. The new unstressed state, O_1, differs from the initial unstressed state, O_0, in that a permanent change in the shape of the bar is observed. This shape change is represented in the graph by the permanent (or *plastic*) axial strain ε^p. Monotonic reloading of the bar to a stress level σ_1 will follow the path $O_1Y_1Z_1$. Similarly to the initial *elastic* segment O_0Y_0, the portion O_1Y_1 is also virtually straight and unloading from Y_1 (or before Y_1 is reached) will bring the stress–strain state back to the unstressed configuration O_1, with no further plastic straining of the bar. Therefore, the behaviour of the material in the segment O_1Y_1 may also be regarded as linear elastic. Here, it is important to emphasise that, even though some discrepancy between unloading and reloading curves (such as lines Z_0O_1 and O_1Y_1) is observed in typical experiments, the actual difference between them is in fact much smaller than that shown in the diagram of Figure 6.1. Again, loading beyond an *elastic limit* (point Y_1 in this case) will cause further increase in plastic deformation.

Some important phenomenological properties can be identified in the above described uniaxial test. They are enumerated below:

1. The existence of an *elastic domain*, i.e. a range of stresses within which the behaviour of the material can be considered as purely elastic, without evolution of permanent (plastic) strains. The elastic domain is delimited by the so-called *yield stress*. In Figure 6.1, segments O_0Y_0 and O_1Y_1 define the elastic domain at two different states. The associated yield stresses correspond to points Y_0 and Y_1.

2. If the material is further loaded at the yield stress, then *plastic yielding* (or *plastic flow*), i.e. evolution of plastic strains, takes place.

3. Accompanying the evolution of the plastic strain, an *evolution of the yield stress* itself is also observed (note that the yield stresses corresponding to points Y_0 and Y_1 are different). This phenomenon is known as *hardening*.

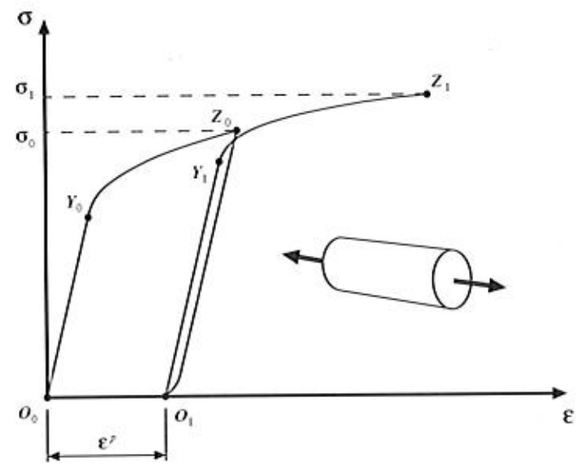

Figure 6.1. Uniaxial tension experiment with ductile metals.

It is emphasised that the above properties can be observed not only in metals but also in a wide variety of materials such as concrete, rocks, soils and many others. Obviously, the microscopic mechanisms that give rise to these common phenomenological characteristics can be completely distinct for different types of material. It is also important to note that, according to the type of material, different experimental procedures may be required for the verification of such properties. For instance, in materials such as soils, which typically cannot resist tensile stresses, uniaxial tension tests do not make physical sense. In this case, experiments such as *triaxial shear tests*, in which the sides of the specimen are subjected to a confining hydrostatic pressure prior to the application of longitudinal compression, are more appropriate.

The object of the mathematical theory of plasticity is to provide continuum constitutive models capable of describing (qualitatively and quantitavely) with sufficient accuracy the phenomenological behaviour of materials that possess the characteristics discussed in the above.

6.2. One-dimensional constitutive model

A simple mathematical model of the uniaxial experiment discussed in the previous section is formulated in what follows. In spite of its simplicity the one-dimensional constitutive model contains all the essential features that form the basis of the mathematical theory of plasticity.

At the outset, the original stress–strain curve of Figure 6.1, that resulted from the loading programme described in the previous section, is approximated by the idealised version shown in Figure 6.2. The assumptions involved in the approximation are summarised in the following. Firstly, the difference between unloading and reloading curves (segments Z_0O_1 and O_1Y_1 of Figure 6.1) is ignored and points Z_0 and Y_1, that correspond respectively to

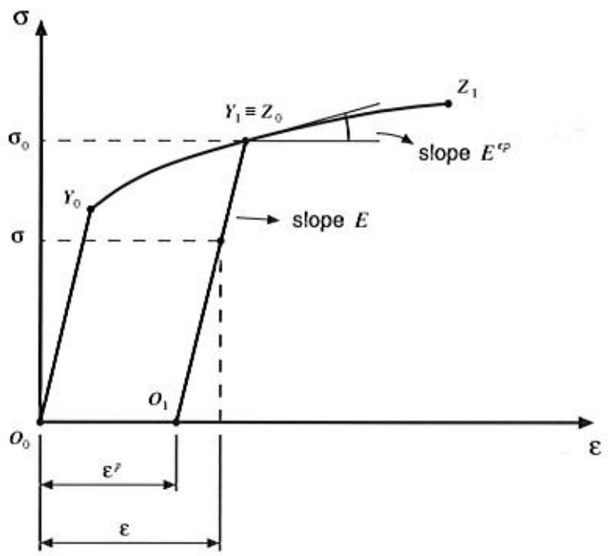

Figure 6.2. Uniaxial tension experiment. Mathematical model.

the beginning of unloading and the onset of plastic yielding upon subsequent reloading, are assumed to coincide. The transition between the elastic region and the elastoplastic regime is now clearly marked by a non-smooth change of slope (points Y_0 and Y_1). During plastic yielding, the stress–strain curve always follows the path defined by $O_0Y_0Y_1Z_1$. This path is normally referred to as the *virgin curve* and is obtained by a continuous monotonic loading from the initial unstressed state O_0.

Under the above assumptions, after being monotonically loaded from the initial unstressed state to the stress level σ_0, the behaviour of the bar between states O_1 and Y_1 is considered to be linear elastic, with constant plastic strain, ε^p, and yield limit, σ_0. Thus, within the segment O_1Y_1, the uniaxial stress corresponding to a configuration with *total* strain ε is given by

$$\sigma = E\,(\varepsilon - \varepsilon^p), \tag{6.1}$$

where E denotes the Young's modulus of the material of the bar. Note that the difference between the total strain and the current plastic strain, $\varepsilon - \varepsilon^p$, is *fully reversible*; that is, upon complete unloading of the bar, $\varepsilon - \varepsilon^p$ is fully recovered without further evolution of plastic strains. This motivates the additive decomposition of the axial strain described in the following section.

6.2.1. ELASTOPLASTIC DECOMPOSITION OF THE AXIAL STRAIN

One of the chief hypotheses underlying the small strain theory of plasticity is the decomposition of the *total strain*, ε, into the sum of an *elastic* (or reversible) component, ε^e, and a

plastic (or permanent) component, ε^p,

$$\varepsilon = \varepsilon^e + \varepsilon^p, \tag{6.2}$$

where the *elastic strain* has been defined as

$$\varepsilon^e = \varepsilon - \varepsilon^p. \tag{6.3}$$

6.2.2. THE ELASTIC UNIAXIAL CONSTITUTIVE LAW

Following the above definition of the elastic axial strain, the constitutive law for the axial stress can be expressed as

$$\sigma = E\,\varepsilon^e. \tag{6.4}$$

The next step in the definition of the uniaxial constitutive model is to derive formulae that express mathematically the fundamental phenomenological properties enumerated in Section 6.1. The items 1 and 2 of Section 6.1 are associated with the formulation of a *yield criterion* and a *plastic flow rule*, whereas item 3 requires the formulation of a *hardening law*. These are described in the following.

6.2.3. THE YIELD FUNCTION AND THE YIELD CRITERION

The existence of an elastic domain delimited by a yield stress has been pointed out in item 1 of Section 6.1. With the introduction of a *yield function*, Φ, of the form

$$\Phi(\sigma, \sigma_y) = |\sigma| - \sigma_y, \tag{6.5}$$

the *elastic domain* at a state with uniaxial yield stress σ_y can be defined in the one-dimensional plasticity model as the set

$$\mathcal{E} = \{\sigma \mid \Phi(\sigma, \sigma_y) < 0\}, \tag{6.6}$$

or, equivalently, the elastic domain is the set of stresses σ that satisfy

$$|\sigma| < \sigma_y. \tag{6.7}$$

Generalising the results of the uniaxial *tension* test discussed, it has been assumed in the above that the yield stress in compression is identical to that in tension. The corresponding idealised elastic domain is illustrated in Figure 6.3.

It should be noted that, at any stage, no stress level is allowed above the current yield stress, i.e. *plastically admissible stresses* lie either in the elastic domain or on its boundary (the yield limit). Thus, any admissible stress must satisfy the restriction

$$\Phi(\sigma, \sigma_y) \leq 0. \tag{6.8}$$

For stress levels within the elastic domain, only elastic straining may occur, whereas on its boundary (at the yield stress), either elastic unloading or plastic yielding (or plastic loading) takes place. This *yield criterion* can be expressed by

$$\begin{aligned} &\text{If } \Phi(\sigma, \sigma_y) < 0 \Longrightarrow \dot{\varepsilon}^p = 0, \\ &\text{If } \Phi(\sigma, \sigma_y) = 0 \Longrightarrow \begin{cases} \dot{\varepsilon}^p = 0 & \text{for elastic unloading,} \\ \dot{\varepsilon}^p \neq 0 & \text{for plastic loading.} \end{cases} \end{aligned} \tag{6.9}$$

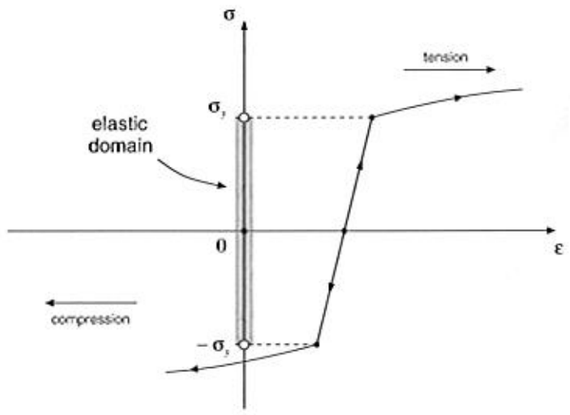

Figure 6.3. Uniaxial model. Elastic domain.

6.2.4. THE PLASTIC FLOW RULE. LOADING/UNLOADING CONDITIONS

Expressions (6.9) above have defined a criterion for plastic yielding, i.e. they have set the conditions under which plastic straining may occur. By noting in Figure 6.3 that, upon plastic loading, the plastic strain rate $\dot{\varepsilon}^p$ is positive (stretching) under tension (positive σ) and negative (compressive) under compression (negative σ), the *plastic flow rule* for the uniaxial model can be formally established as

$$\dot{\varepsilon}^p = \dot{\gamma}\,\mathrm{sign}(\sigma), \tag{6.10}$$

where sign is the *signum* function defined as

$$\mathrm{sign}(a) = \begin{cases} +1 & \text{if } a \geq 0 \\ -1 & \text{if } a < 0 \end{cases} \tag{6.11}$$

for any scalar a and the scalar $\dot{\gamma}$ is termed the *plastic multiplier*. The plastic multiplier is *non-negative*,

$$\dot{\gamma} \geq 0, \tag{6.12}$$

and satisfies the *complementarity condition*

$$\Phi\,\dot{\gamma} = 0. \tag{6.13}$$

The constitutive equations (6.10) to (6.13) imply that, as stated in the yield criterion (6.9), the plastic strain rate vanishes within the elastic domain, i.e.

$$\Phi < 0 \implies \dot{\gamma} = 0 \implies \dot{\varepsilon}^p = 0, \tag{6.14}$$

and plastic flow ($\dot{\varepsilon}^p \neq 0$) may occur only when the stress level σ coincides with the current yield stress

$$|\sigma| = \sigma_y \implies \Phi = 0 \implies \dot{\gamma} \geq 0. \tag{6.15}$$

Expressions (6.8), (6.12) and (6.13) define the so-called *loading/unloading conditions* of the elasticplastic model; that is, the constraints

$$\Phi \leq 0, \quad \dot{\gamma} \geq 0, \quad \dot{\gamma}\Phi = 0, \tag{6.16}$$

establish when plastic flow may occur.

6.2.5. THE HARDENING LAW

Finally, the complete characterisation of the uniaxial model is achieved with the introduction of the *hardening law*. As remarked in item 3 of Section 6.1, an evolution of the yield stress accompanies the evolution of the plastic strain. This phenomenon, known as *hardening*, can be incorporated into the uniaxial model simply by assuming that, in the definition (6.5) of Φ, the yield stress σ_y is a given function

$$\sigma_y = \sigma_y(\bar{\varepsilon}^p) \tag{6.17}$$

of the *accumulated* axial plastic strain, $\bar{\varepsilon}^p$. The accumulated axial plastic strain is defined as

$$\bar{\varepsilon}^p \equiv \int_0^t |\dot{\varepsilon}^p|\,\mathrm{d}t, \tag{6.18}$$

thus ensuring that both tensile and compressive plastic straining contribute to $\bar{\varepsilon}^p$. Clearly, in a monotonic tensile test we have

$$\bar{\varepsilon}^p = \varepsilon^p, \tag{6.19}$$

whereas in a monotonic compressive uniaxial test,

$$\bar{\varepsilon}^p = -\varepsilon^p. \tag{6.20}$$

The curve defined by the hardening function $\sigma_y(\bar{\varepsilon}^p)$ is usually referred to as the *hardening curve* (Figure 6.4).

From the definition of $\bar{\varepsilon}^p$, it follows that its evolution law is given by

$$\dot{\bar{\varepsilon}}^p = |\dot{\varepsilon}^p|, \tag{6.21}$$

which, in view of the plastic flow rule, is equivalent to

$$\dot{\bar{\varepsilon}}^p = \dot{\gamma}. \tag{6.22}$$

6.2.6. SUMMARY OF THE MODEL

The overall one-dimensional plasticity model is defined by the constitutive equations (6.2), (6.4), (6.5), (6.10), (6.16), (6.17), and (6.22). The model is summarised in Box 6.1.

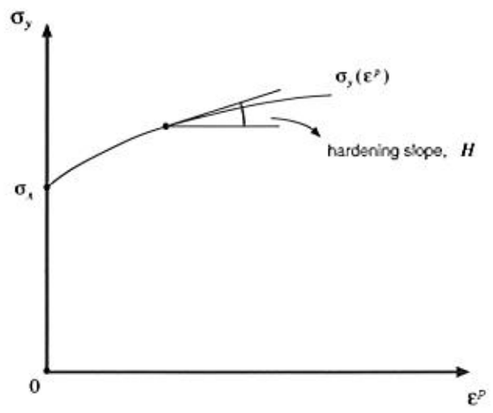

Figure 6.4. One-dimensional model. Hardening curve.

Box 6.1. One-dimensional elastoplastic constitutive model.

1. Elastoplastic split of the axial strain

$$\varepsilon = \varepsilon^e + \varepsilon^p$$

2. Uniaxial elastic law

$$\sigma = E\,\varepsilon^e$$

3. Yield function

$$\Phi(\sigma, \sigma_y) = |\sigma| - \sigma_y$$

4. Plastic flow rule

$$\dot{\varepsilon}^p = \dot{\gamma}\,\mathrm{sign}(\sigma)$$

5. Hardening law

$$\sigma_y = \sigma_y(\bar{\varepsilon}^p)$$

$$\dot{\bar{\varepsilon}}^p = \dot{\gamma}$$

6. Loading/unloading criterion

$$\Phi \le 0, \quad \dot{\gamma} \ge 0, \quad \dot{\gamma}\Phi = 0$$

6.2.7. DETERMINATION OF THE PLASTIC MULTIPLIER

So far, in the uniaxial plasticity model introduced above, the *plastic multiplier*, $\dot{\gamma}$, was left indeterminate during plastic yielding. Indeed, expressions (6.12) and (6.13) just tell us that $\dot{\gamma}$ vanishes during elastic straining but may assume *any* non-negative value during plastic flow. In order to eliminate this indetermination, it should be noted firstly that, *during plastic flow*,

the value of the yield function remains constant

$$\Phi = 0, \tag{6.23}$$

as the absolute value of the current stress always coincides with the current yield stress. Therefore, the following additional complementarity condition may be established:

$$\dot{\Phi}\,\dot{\gamma} = 0 \tag{6.24}$$

which implies that the rate of Φ vanishes whenever plastic yielding occurs ($\dot{\gamma} \neq 0$),

$$\dot{\Phi} = 0, \tag{6.25}$$

and, during elastic straining, ($\dot{\gamma} = 0$), $\dot{\Phi}$ may assume any value. Equation (6.25) is called the *consistency condition*. By taking the time derivative of the yield function (6.5), one obtains

$$\dot{\Phi} = \mathrm{sign}(\sigma)\,\dot{\sigma} - H\,\dot{\bar{\varepsilon}}^p, \tag{6.26}$$

where H is called the *hardening modulus*, or *hardening slope*, and is defined as (refer to Figure 6.4)

$$H = H(\bar{\varepsilon}^p) = \frac{\mathrm{d}\sigma_y}{\mathrm{d}\bar{\varepsilon}^p}. \tag{6.27}$$

Under plastic yielding, equation (6.25) holds so that one has the following expression for the stress rate

$$\mathrm{sign}(\sigma)\,\dot{\sigma} = H\,\dot{\bar{\varepsilon}}^p. \tag{6.28}$$

From the elastic law, it follows that

$$\dot{\sigma} = E(\dot{\varepsilon} - \dot{\varepsilon}^p). \tag{6.29}$$

Finally, by combining the above expression with (6.22), (6.28) and (6.10), the plastic multiplier, $\dot{\gamma}$, is *uniquely* determined during plastic yielding as

$$\dot{\gamma} = \frac{E}{H+E}\,\mathrm{sign}(\sigma)\,\dot{\varepsilon} = \frac{E}{H+E}\,|\dot{\varepsilon}|. \tag{6.30}$$

6.2.8. THE ELASTOPLASTIC TANGENT MODULUS

Let us now return to the stress–strain curve of Figure 6.2. Plastic flow at a generic yield limit produces the following tangent relation between strain and stress

$$\dot{\sigma} = E^{ep}\,\dot{\varepsilon}, \tag{6.31}$$

where E^{ep} is called the *elastoplastic tangent modulus*. By combining expressions (6.31), (6.29), the flow rule (6.10) and (6.30) the following expression is obtained for the elastoplastic tangent modulus

$$E^{ep} = \frac{E\,H}{E+H}. \tag{6.32}$$

Equivalently, the hardening modulus, H, can be expressed in terms of the elastic modulus and the elastoplastic modulus as

$$H = \frac{E^{ep}}{1 - E^{ep}/E}. \tag{6.33}$$

6.3. General elastoplastic constitutive model

A mathematical model of a uniaxial tension experiment with a ductile metal has been described in the previous section. As already mentioned, the one-dimensional equations contain all basic components of a general elastoplastic constitutive model:

- the elastoplastic strain decomposition;
- an elastic law;
- a yield criterion, stated with the use of a yield function;
- a plastic flow rule defining the evolution of the plastic strain; and
- a hardening law, characterising the evolution of the yield limit.

The generalisation of these concepts for application in two- and three-dimensional situations is described in this section.

6.3.1. ADDITIVE DECOMPOSITION OF THE STRAIN TENSOR

Following the decomposition of the uniaxial strain given in the previous section, the corresponding generalisation is obtained by splitting the strain *tensor*, $\boldsymbol{\varepsilon}$, into the sum of an elastic component, $\boldsymbol{\varepsilon}^e$, and a plastic component, $\boldsymbol{\varepsilon}^p$; that is,

$$\boldsymbol{\varepsilon} = \boldsymbol{\varepsilon}^e + \boldsymbol{\varepsilon}^p. \tag{6.34}$$

The tensors $\boldsymbol{\varepsilon}^e$ and $\boldsymbol{\varepsilon}^p$ are known, respectively, as the *elastic strain tensor* and the *plastic strain tensor*. The corresponding rate form of the additive split reads

$$\dot{\boldsymbol{\varepsilon}} = \dot{\boldsymbol{\varepsilon}}^e + \dot{\boldsymbol{\varepsilon}}^p. \tag{6.35}$$

Note that (6.35) together with the given initial condition

$$\boldsymbol{\varepsilon}(t_0) = \boldsymbol{\varepsilon}^e(t_0) + \boldsymbol{\varepsilon}^p(t_0) \tag{6.36}$$

at a (pseudo-)time t_0 is equivalent to (6.34).

6.3.2. THE FREE ENERGY POTENTIAL AND THE ELASTIC LAW

The formulation of general dissipative models of solids within the framework of thermodynamics with an internal variable has been addressed in Section 3.5 of Chapter 3. Recall that the free energy potential plays a crucial role in the derivation of the model and provides the constitutive law for stress. The starting point of the theories of plasticity treated in this book is the assumption that the free energy, ψ, is a function

$$\psi(\boldsymbol{\varepsilon}, \boldsymbol{\varepsilon}^p, \boldsymbol{\alpha}),$$

of the total strain, the plastic strain (taken as an internal variable) and a set $\boldsymbol{\alpha}$ of internal variables associated with the phenomenon of hardening. It is usual to assume that the free

energy can be split as

$$\begin{aligned}\psi(\boldsymbol{\varepsilon}, \boldsymbol{\varepsilon}^p, \boldsymbol{\alpha}) &= \psi^e(\boldsymbol{\varepsilon} - \boldsymbol{\varepsilon}^p) + \psi^p(\boldsymbol{\alpha}) \\ &= \psi^e(\boldsymbol{\varepsilon}^e) + \psi^p(\boldsymbol{\alpha})\end{aligned} \tag{6.37}$$

into a sum of an elastic contribution, ψ^e, whose dependence upon strains and internal variables appears only through the elastic strain, and a contribution due to hardening, ψ^p.

Following the above expression for the free energy, the Clausius–Duhem inequality reads

$$\left(\boldsymbol{\sigma} - \bar{\rho}\,\frac{\partial \psi^e}{\partial \boldsymbol{\varepsilon}^e}\right) : \dot{\boldsymbol{\varepsilon}}^e + \boldsymbol{\sigma} : \dot{\boldsymbol{\varepsilon}}^p - \boldsymbol{A} * \dot{\boldsymbol{\alpha}} \geq 0, \tag{6.38}$$

where

$$\boldsymbol{A} \equiv \bar{\rho}\,\partial \psi^p / \partial \boldsymbol{\alpha} \tag{6.39}$$

is the *hardening thermodynamical force* and we note that $-\boldsymbol{\sigma}$ is the thermodynamical force associated with the plastic strain while the symbol * indicates the appropriate product between $\boldsymbol{A}$ and $\dot{\boldsymbol{\alpha}}$. The above inequality implies a general elastic law of the form

$$\boldsymbol{\sigma} = \bar{\rho}\,\frac{\partial \psi^e}{\partial \boldsymbol{\varepsilon}^e}, \tag{6.40}$$

so that the requirement of non-negative dissipation can be reduced to

$$\Upsilon^p(\boldsymbol{\sigma}, \boldsymbol{A}; \dot{\boldsymbol{\varepsilon}}^p, \dot{\boldsymbol{\alpha}}) \geq 0, \tag{6.41}$$

where the function Υ^p, defined by

$$\Upsilon^p(\boldsymbol{\sigma}, \boldsymbol{A}; \dot{\boldsymbol{\varepsilon}}^p, \dot{\boldsymbol{\alpha}}) \equiv \boldsymbol{\sigma} : \dot{\boldsymbol{\varepsilon}}^p - \boldsymbol{A} * \dot{\boldsymbol{\alpha}}, \tag{6.42}$$

is called the *plastic dissipation function*.

This chapter is focused on materials whose elastic behaviour is *linear* (as in the uniaxial model of the previous section) and isotropic. In this case, the elastic contribution to the free energy is given by

$$\begin{aligned}\bar{\rho}\,\psi^e(\boldsymbol{\varepsilon}^e) &= \tfrac{1}{2}\,\boldsymbol{\varepsilon}^e : \mathbf{D}^e : \boldsymbol{\varepsilon}^e \\ &= G\,\boldsymbol{\varepsilon}^e_d : \boldsymbol{\varepsilon}^e_d + \tfrac{1}{2}\,K\,(\varepsilon^e_v)^2\end{aligned} \tag{6.43}$$

where $\mathbf{D}^e$ is the standard isotropic elasticity tensor and G and K are, respectively the shear and bulk moduli. The tensor $\boldsymbol{\varepsilon}^e_d$ is the deviatoric component of the elastic strain and $\varepsilon^e_v \equiv \mathrm{tr}[\boldsymbol{\varepsilon}^e]$ is the volumetric elastic strain. Thus, the general counterpart of uniaxial elastic law (6.4) is given by

$$\begin{aligned}\boldsymbol{\sigma} &= \mathbf{D}^e : \boldsymbol{\varepsilon}^e \\ &= 2G\,\boldsymbol{\varepsilon}^e_d + K\,\varepsilon^e_v\,\boldsymbol{I}.\end{aligned} \tag{6.44}$$

6.3.3. THE YIELD CRITERION AND THE YIELD SURFACE

Recall that in the uniaxial yield criterion it was established that plastic flow may occur when the uniaxial stress attains a critical value. This principle could be expressed by means of a yield function which is negative when only elastic deformations are possible and reaches zero when plastic flow is imminent. Extension of this concept to the three-dimensional case is obtained by stating that plastic flow may occur only when

$$\Phi(\boldsymbol{\sigma}, \boldsymbol{A}) = 0, \tag{6.45}$$

where the scalar yield function, Φ, is now a function of the stress *tensor* and a set $\boldsymbol{A}$ of hardening thermodynamical forces. Analogously to the uniaxial case, a yield function defines the *elastic domain* as the set

$$\mathscr{E} = \{\boldsymbol{\sigma} \mid \Phi(\boldsymbol{\sigma}, \boldsymbol{A}) < 0\} \tag{6.46}$$

of stresses for which plastic yielding is not possible. Any stress lying in the elastic domain or on its boundary is said to be *plastically admissible*. We then define the *set of plastically admissible stresses* (or *plastically admissible domain*) as

$$\bar{\mathscr{E}} = \{\boldsymbol{\sigma} \mid \Phi(\boldsymbol{\sigma}, \boldsymbol{A}) \leq 0\}. \tag{6.47}$$

The yield locus, i.e. the set of stresses for which plastic yielding may occur, is the boundary of the elastic domain, where $\Phi(\boldsymbol{\sigma}, \boldsymbol{A}) = 0$. The yield locus in this case is represented by a hypersurface in the space of stresses. This hypersurface is termed the *yield surface* and is defined as

$$\mathscr{Y} = \{\boldsymbol{\sigma} \mid \Phi(\boldsymbol{\sigma}, \boldsymbol{A}) = 0\}. \tag{6.48}$$

6.3.4. PLASTIC FLOW RULE AND HARDENING LAW

The complete characterisation of the general plasticity model requires the definition of the evolution laws for the internal variables, i.e. the variables associated with the dissipative phenomena. In the present case, the internal variables are the plastic strain tensor and the set $\boldsymbol{\alpha}$ of hardening variables. The following plastic flow rule and hardening law are then postulated

$$\dot{\boldsymbol{\varepsilon}}^p = \dot{\gamma}\, \boldsymbol{N} \tag{6.49}$$

$$\dot{\boldsymbol{\alpha}} = \dot{\gamma}\, \boldsymbol{H}, \tag{6.50}$$

where the tensor

$$\boldsymbol{N} = \boldsymbol{N}(\boldsymbol{\sigma}, \boldsymbol{A}) \tag{6.51}$$

is termed the *flow vector* and the function

$$\boldsymbol{H} = \boldsymbol{H}(\boldsymbol{\sigma}, \boldsymbol{A}) \tag{6.52}$$

is the *generalised hardening modulus* which defines the evolution of the hardening variables. The evolution equations (6.49) and (6.50) are complemented by the loading/unloading conditions

$$\Phi \leq 0, \quad \dot{\gamma} \geq 0, \quad \Phi\dot{\gamma} = 0, \tag{6.53}$$

that define when evolution of plastic strains and internal variables ($\dot{\gamma} \neq 0$) may occur.

For convenience, the general plasticity model resulting from the above equations is listed in Box 6.2.

Box 6.2. A general elastoplastic constitutive model.

1. Additive decomposition of the strain tensor

$$\boldsymbol{\varepsilon} = \boldsymbol{\varepsilon}^e + \boldsymbol{\varepsilon}^p$$

or

$$\dot{\boldsymbol{\varepsilon}} = \dot{\boldsymbol{\varepsilon}}^e + \dot{\boldsymbol{\varepsilon}}^p, \quad \boldsymbol{\varepsilon}(t_0) = \boldsymbol{\varepsilon}^e(t_0) + \boldsymbol{\varepsilon}^p(t_0)$$

2. Free-energy function

$$\psi = \psi(\boldsymbol{\varepsilon}^e, \boldsymbol{\alpha})$$

where $\boldsymbol{\alpha}$ is a set of hardening internal variables

3. Constitutive equation for $\boldsymbol{\sigma}$ and hardening thermodynamic forces $\boldsymbol{A}$

$$\boldsymbol{\sigma} = \bar{\rho}\, \frac{\partial \psi}{\partial \boldsymbol{\varepsilon}^e}, \quad \boldsymbol{A} = \bar{\rho}\, \frac{\partial \psi}{\partial \boldsymbol{\alpha}}$$

4. Yield function

$$\Phi = \Phi(\boldsymbol{\sigma}, \boldsymbol{A})$$

5. Plastic flow rule and hardening law

$$\dot{\boldsymbol{\varepsilon}}^p = \dot{\gamma}\, \boldsymbol{N}(\boldsymbol{\sigma}, \boldsymbol{A})$$

$$\dot{\boldsymbol{\alpha}} = \dot{\gamma}\, \boldsymbol{H}(\boldsymbol{\sigma}, \boldsymbol{A})$$

6. Loading/unloading criterion

$$\Phi \leq 0, \quad \dot{\gamma} \geq 0, \quad \dot{\gamma}\Phi = 0$$

6.3.5. FLOW RULES DERIVED FROM A FLOW POTENTIAL

In the formulation of multidimensional plasticity models, it is often convenient to define the flow rule (and possibly the hardening law) in terms of a *flow* (or *plastic*) *potential*. The starting point of such an approach is to postulate the existence of a flow potential with general form

$$\Psi = \Psi(\boldsymbol{\sigma}, \boldsymbol{A}) \tag{6.54}$$

from which the flow vector, $\boldsymbol{N}$, is obtained as

$$\boldsymbol{N} \equiv \frac{\partial \Psi}{\partial \boldsymbol{\sigma}}. \tag{6.55}$$

If the hardening law is assumed to be derived from the same potential, then we have in addition

$$\boldsymbol{H} \equiv -\frac{\partial \Psi}{\partial \boldsymbol{A}}. \tag{6.56}$$

When such an approach is adopted, the plastic potential, Ψ, is required to be a non-negative convex function of both $\boldsymbol{\sigma}$ and $\boldsymbol{A}$ and zero-valued at the origin,

$$\Psi(\boldsymbol{0}, \boldsymbol{0}) = 0. \tag{6.57}$$

These restrictions ensure that the dissipation inequality (6.41) is satisfied *a priori* by the evolution equations (6.49) and (6.50).

Associative flow rule

As we shall see later, many plasticity models, particularly for ductile metals, have their yield function, Φ, as a flow potential, i.e.

$$\Psi \equiv \Phi. \tag{6.58}$$

Such models are called *associative* (or *associated*) plasticity models. The issue of associativity will be further discussed in Section 6.5.1.

6.3.6. THE PLASTIC MULTIPLIER

Here we extend to the multidimensional case the procedure for the determination of the plastic multiplier, $\dot{\gamma}$, described in Section 6.2.7 for the one-dimensional plasticity model. Following the same arguments employed in Section 6.2.7, the starting point in the determination of $\dot{\gamma}$ is the consideration of the additional complementarity equation

$$\dot{\Phi}\,\dot{\gamma} = 0, \tag{6.59}$$

which implies the *consistency condition*

$$\dot{\Phi} = 0 \tag{6.60}$$

under plastic yielding (when $\dot{\gamma} \neq 0$). By differentiating the yield function with respect to time, we obtain

$$\dot{\Phi} = \frac{\partial \Phi}{\partial \boldsymbol{\sigma}} : \dot{\boldsymbol{\sigma}} + \frac{\partial \Phi}{\partial A} * \dot{A}. \tag{6.61}$$

By taking into account the additive split of the strain tensor, the elastic law and the plastic flow rule (6.49), we promptly find the obvious rate form

$$\dot{\boldsymbol{\sigma}} = \mathbf{D}^e : (\dot{\boldsymbol{\varepsilon}} - \dot{\boldsymbol{\varepsilon}}^p) = \mathbf{D}^e : (\dot{\boldsymbol{\varepsilon}} - \dot{\gamma}\, \boldsymbol{N}). \tag{6.62}$$

This, together with the definition of A in terms of the free-energy potential (refer to expression (6.39)) and the evolution law (6.50), allow us to write (6.61) equivalently as

$$\begin{aligned} \dot{\Phi} &= \frac{\partial \Phi}{\partial \boldsymbol{\sigma}} : \mathbf{D}^e : (\dot{\boldsymbol{\varepsilon}} - \dot{\boldsymbol{\varepsilon}}^p) + \frac{\partial \Phi}{\partial A} * \bar{\rho} \frac{\partial^2 \psi^p}{\partial \boldsymbol{\alpha}^2} * \dot{\boldsymbol{\alpha}}. \\ &= \frac{\partial \Phi}{\partial \boldsymbol{\sigma}} : \mathbf{D}^e : (\dot{\boldsymbol{\varepsilon}} - \dot{\gamma}\, \boldsymbol{N}) + \dot{\gamma}\, \frac{\partial \Phi}{\partial A} * \bar{\rho} \frac{\partial^2 \psi^p}{\partial \boldsymbol{\alpha}^2} * \boldsymbol{H}. \end{aligned} \tag{6.63}$$

Finally, the above expression and the consistency condition (6.60) lead to the following closed formula for the plastic multiplier

$$\dot{\gamma} = \frac{\partial \Phi / \partial \boldsymbol{\sigma} : \mathbf{D}^e : \dot{\boldsymbol{\varepsilon}}}{\partial \Phi / \partial \boldsymbol{\sigma} : \mathbf{D}^e : \boldsymbol{N} - \partial \Phi / \partial A * \bar{\rho} \partial^2 \psi^p / \partial \boldsymbol{\alpha}^2 * \boldsymbol{H}}. \tag{6.64}$$

6.3.7. RELATION TO THE GENERAL CONTINUUM CONSTITUTIVE THEORY

At this point, we should emphasise that the general rate-independent plasticity model described above can under some conditions be shown to be a particular instance of the general constitutive theory postulated in Section 3.5.2, starting page 71. The link between the two theories can be clearly demonstrated when rate-independent plasticity is obtained as a limit case of rate-dependent plasticity (or viscoplasticity).

However, since the theory of elasto-viscoplasticity is introduced only in Chapter 11, we find it convenient to carry on focusing on rate-independent plasticity and postpone the demonstration until that chapter. Those wishing to see now the link between rate-independent plasticity and the general constitutive theory are referred to Section 11.4.3, starting on page 452. We remark, though, that the concept of subdifferential, introduced below in Section 6.3.9, is fundamental to the demonstration. Readers not yet familiar with this concept are advised to read through Section 6.3.9 before moving to Section 11.4.3.

6.3.8. RATE FORM AND THE ELASTOPLASTIC TANGENT OPERATOR

In the elastic regime, the rate constitutive equation for stress reads simply

$$\dot{\boldsymbol{\sigma}} = \mathbf{D}^e : \dot{\boldsymbol{\varepsilon}}. \tag{6.65}$$

Under plastic flow, the corresponding rate relation can be obtained by introducing expression (6.64) into (6.62). The rate equation reads

$$\dot{\boldsymbol{\sigma}} = \mathbf{D}^{ep} : \dot{\boldsymbol{\varepsilon}}, \tag{6.66}$$

where $\mathbf{D}^{ep}$ is the *elastoplastic tangent modulus* given by

$$\mathbf{D}^{ep} = \mathbf{D}^e - \frac{(\mathbf{D}^e : \boldsymbol{N}) \otimes (\mathbf{D}^e : \partial \Phi / \partial \boldsymbol{\sigma})}{\partial \Phi / \partial \boldsymbol{\sigma} : \mathbf{D}^e : \boldsymbol{N} - \partial \Phi / \partial A * \bar{\rho} \partial^2 \psi^p / \partial \boldsymbol{\alpha}^2 * \boldsymbol{H}}. \tag{6.67}$$

In obtaining the above expression, we have made use of the fact that the symmetry (refer to equation (2.87), page 29) of the elasticity tensor implies

$$\partial \Phi / \partial \boldsymbol{\sigma} : \mathbf{D}^e : \dot{\boldsymbol{\varepsilon}} = \mathbf{D}^e : \partial \Phi / \partial \boldsymbol{\sigma} : \dot{\boldsymbol{\varepsilon}}. \tag{6.68}$$

The fourth-order tensor $\mathbf{D}^{ep}$ is the multidimensional generalisation of the scalar modulus E^{ep} associated with the slope of the uniaxial stress–strain curve under plastic flow. In the computational plasticity literature, $\mathbf{D}^{ep}$ is frequently referred to as the *continuum* elastoplastic tangent operator.

Remark 6.1 (The symmetry of $\mathbf{D}^{ep}$). Note that if the plastic flow rule is *associative*, i.e. if $\boldsymbol{N} \equiv \partial \Phi / \partial \boldsymbol{\sigma}$, then the continuum elastoplastic tangent operator is *symmetric*. For models with non-associative plastic flow, $\mathbf{D}^{ep}$ is generally unsymmetric.

6.3.9. NON-SMOOTH POTENTIALS AND THE SUBDIFFERENTIAL

It should be noted that expressions (6.55) and (6.56) only make sense if the potential Ψ is differentiable. When that happens, the flow vector, $\boldsymbol{N}$, can be interpreted as a vector

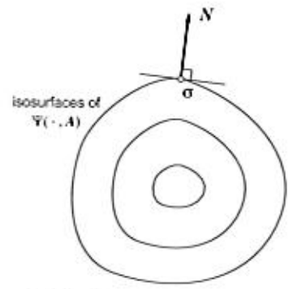

Figure 6.5. The flow vector. Smooth potential.

normal to the iso-surfaces of function Ψ in the space of stresses (with fixed $\boldsymbol{A}$). A schematic representation of $\boldsymbol{N}$ in this case is shown in Figure 6.5. The generalised modulus, H, can be interpreted in a completely analogous way.

The requirement of differentiability of the flow potential is, however, too restrictive and many practical plasticity models are based on the use of a non-differentiable Ψ. Specific examples are given later in this chapter. For a more comprehensive account of such theories the reader is referred to Duvaut and Lions (1976), Eve *et al.* (1990) and Han and Reddy (1999). In such cases, the function Ψ is called a *pseudo-potential* or *generalised potential* and the formulation of the evolution laws for the internal variables can be dealt with by introducing the concept of *subdifferential sets*, which generalises the classical definition of derivative.[†]

Subgradients and the subdifferential

Let us consider a *scalar* function $y : \mathscr{R}^n \to \mathscr{R}$. The *subdifferential* of y at a point $\bar{\boldsymbol{x}}$ is the set

$$\partial y(\bar{\boldsymbol{x}}) = \{s \in \mathscr{R}^n \mid y(\boldsymbol{x}) - y(\bar{\boldsymbol{x}}) \geq \boldsymbol{s} \cdot (\boldsymbol{x} - \bar{\boldsymbol{x}}),\ \forall\, \boldsymbol{x} \in \mathscr{R}^n\}. \tag{6.69}$$

If the set ∂y is not empty at $\bar{\boldsymbol{x}}$, the function y is said to be *subdifferentiable* at $\bar{\boldsymbol{x}}$. The elements of ∂y are called *subgradients* of y. If the function y is *differentiable*, then the subdifferential contains a *unique* subgradient which coincides with the derivative of y,

$$\partial y = \left\{\frac{\mathrm{d}y}{\mathrm{d}\boldsymbol{x}}\right\}. \tag{6.70}$$

A schematic illustration of the concept of subdifferential is shown in Figure 6.6 for $n = 1$. In this case, when y is subdifferentiable (but not necessarily differentiable) at a point $\bar{x}$, the subdifferential at that point is composed of all slopes s lying between the slopes on the right and left of $\bar{x}$ (the two one-sided derivatives of y at $\bar{x}$).

[†]The concept of subdifferential sets is exploited extensively in convex analysis. The reader is referred to Rockafellar (1970), Part V, for a detailed account of the theory of subdifferentiable functions.

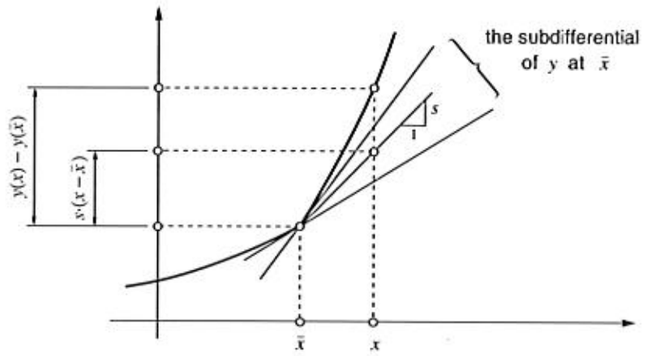

Figure 6.6. The subdifferential of a convex function.

Plastic flow with subdifferentiable flow potentials

Assume now that the (pseudo-) potential Ψ is a subdifferentiable function of $\boldsymbol{\sigma}$ and $\boldsymbol{A}$. At points where Ψ is non-differentiable in $\boldsymbol{\sigma}$, the isosurfaces of Ψ in the space of stresses contain a singularity (corner) where the normal direction is not uniquely defined. A typical situation is schematically illustrated in Figure 6.7 where two distinct normals, $\boldsymbol{N}_1$ and $\boldsymbol{N}_2$, are assumed to exist. In this case, the subdifferential of Ψ with respect to $\boldsymbol{\sigma}$, denoted $\partial_{\boldsymbol{\sigma}}\Psi$, is the set of vectors contained in the cone defined by all linear combinations (with positive coefficients) of $\boldsymbol{N}_1$ and $\boldsymbol{N}_2$. The generalisation of the plastic flow rule (6.49) is obtained by replacing expression (6.55) for the flow vector with

$$\boldsymbol{N} \in \partial_{\boldsymbol{\sigma}}\Psi, \tag{6.71}$$

i.e. the flow vector $\boldsymbol{N}$ is now assumed to be a *subgradient* of Ψ. Analogously, the evolution law (6.50) for $\boldsymbol{\alpha}$ can be generalised with the replacement of the definition (6.56) by

$$\boldsymbol{H} \in -\partial_{\boldsymbol{A}}\Psi. \tag{6.72}$$

At this point, it should be remarked that differentiability of Ψ with respect to the stress tensor is violated for some very basic plasticity models, such as the Tresca, Mohr–Coulomb and Drucker–Prager theories to be seen later. Therefore, the concepts of subgradient and subdifferential sets introduced above are important in the formulation of evolution laws for $\boldsymbol{\varepsilon}^p$.

An alternative definition of the plastic flow rule with non-smooth potentials, which incorporates a wide class of models, is obtained as follows. Firstly assume that a *finite* number, n, of distinct normals $(\boldsymbol{N}_1, \boldsymbol{N}_2, \ldots, \boldsymbol{N}_n)$ is defined at a generic singular point of an isosurface of Ψ. In this case, any subgradient of Ψ can be written as a linear combination

$$c_1\boldsymbol{N}_1 + c_2\boldsymbol{N}_2 + \cdots + c_n\boldsymbol{N}_n,$$

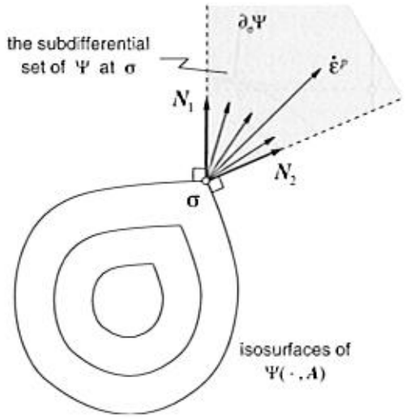

Figure 6.7. The flow vector. Non-smooth potential.

with *non-negative* coefficients $c_1, c_2, \ldots, c_n$.[‡] Based on this observation, the flow rule (6.49) can be generalised as

$$\dot{\varepsilon}^p = \sum_{i=1}^{n} \dot{\gamma}_i N_i, \tag{6.73}$$

with all n plastic multipliers required to be non-negative

$$\dot{\gamma}_i \geq 0, \quad i = 1, \ldots, n. \tag{6.74}$$

The generalisation of the plastic flow law, in this format, was originally proposed by Koiter (1953).

Multisurface models

The above concepts are particularly useful in defining evolution laws for *multisurface* plasticity models. In a generic multisurface model, the elastic domain is bound by a *set* of n surfaces in the space of stresses which intersect in a non-smooth fashion. In this case, n yield functions (Φ_i, $i = 1, \ldots, n$) are defined so that each bounding surface is given by an equation

$$\Phi_i(\boldsymbol{\sigma}, \boldsymbol{A}) = 0. \tag{6.75}$$

The elastic domain in this case reads

$$\mathscr{E} = \{\boldsymbol{\sigma} \mid \Phi_i(\boldsymbol{\sigma}, \boldsymbol{A}) < 0, \ i = 1, \ldots, n\}, \tag{6.76}$$

and the yield surface, i.e. the boundary of $\mathscr{E}$, is the set of all stresses such that $\Phi_i(\boldsymbol{\sigma}, \boldsymbol{A}) = 0$ for at least one i and $\Phi_j(\boldsymbol{\sigma}, \boldsymbol{A}) \leq 0$ for all other indices $j \neq i$.

[‡] It should be emphasised that this representation is not valid for certain types of singularity where the corresponding subdifferential set cannot be generated by a finite number of vectors.

Assuming associativity ($\Psi \equiv \Phi$), the situation discussed previously, where the subgradient of the flow potential is a linear combination of a finite number of normals, is recovered. Thus, the plastic flow rule can be written in the general form (6.73) with the normals being defined here as

$$N_i = \frac{\partial \Phi_i}{\partial \boldsymbol{\sigma}}. \tag{6.77}$$

In the present case, the standard loading/unloading criterion (6.53) is replaced by the generalisation

$$\Phi_i \leq 0, \quad \dot{\gamma}_i \geq 0, \quad \Phi_i \dot{\gamma}_i = 0, \tag{6.78}$$

which must hold for each $i = 1, \ldots, n$. Note that summation on repeated indices is not implied in the above law.

6.4. Classical yield criteria

The general constitutive model for elastoplastic materials has been established in the previous section. There, the yield criterion has been stated in its general form, without reference to any particular criteria. In this section, some of the most common yield criteria used in engineering practice are described in detail; namely, the criteria of *Tresca*, *von Mises*, *Mohr–Coulomb* and *Drucker–Prager*.

6.4.1. THE TRESCA YIELD CRITERION

This criterion was proposed by Tresca (1868) to describe plastic yielding in metals. The Tresca yield criterion assumes that *plastic yielding begins when the maximum shear stress reaches a critical value*.

Recall the spectral representation of the stress tensor,

$$\boldsymbol{\sigma} = \sum_{i=1}^{3} \sigma_i \, \boldsymbol{e}_i \otimes \boldsymbol{e}_i, \tag{6.79}$$

where σ_i are the *principal stresses* and $\boldsymbol{e}_i$ the associated unit eigenvectors, and let $\sigma_{\max}$ and $\sigma_{\min}$ be, respectively, the maximum and minimum principal stresses

$$\begin{aligned} \sigma_{\max} &= \max(\sigma_1, \sigma_2, \sigma_3); \\ \sigma_{\min} &= \min(\sigma_1, \sigma_2, \sigma_3). \end{aligned} \tag{6.80}$$

The *maximum shear stress*, $\tau_{\max}$, is given by

$$\tau_{\max} = \tfrac{1}{2}(\sigma_{\max} - \sigma_{\min}). \tag{6.81}$$

According to the Tresca criterion, the onset of plastic yielding is defined by the condition

$$\tfrac{1}{2}(\sigma_{\max} - \sigma_{\min}) = \tau_y(\alpha), \tag{6.82}$$

where τ_y is the *shear yield stress*, here assumed to be a function of a *hardening internal variable*, α, to be defined later. The shear yield stress is the yield limit under a state of pure shear.

In view of (6.82), the yield function associated with the Tresca yield criterion can be represented as

$$\Phi(\boldsymbol{\sigma}) = \tfrac{1}{2}(\sigma_{\max} - \sigma_{\min}) - \tau_y(\alpha), \tag{6.83}$$

with the onset of yielding characterised by $\Phi = 0$. Alternatively, the Tresca yield function may be defined as

$$\Phi(\boldsymbol{\sigma}) = (\sigma_{\max} - \sigma_{\min}) - \sigma_y(\alpha), \tag{6.84}$$

where σ_y is the *uniaxial* yield stress

$$\sigma_y = 2\,\tau_y, \tag{6.85}$$

that is, it is the stress level at which plastic yielding begins under *uniaxial* stress conditions. That σ_y is indeed the uniaxial yield stress for the Tresca theory can be established by noting that, when plastic yielding begins under uniaxial stress conditions, we have

$$\sigma_{\max} = \sigma_y, \quad \sigma_{\min} = 0. \tag{6.86}$$

The substitution of the above into (6.82) gives (6.85). The elastic domain for the Tresca criterion can be defined as

$$\mathcal{E} = \{\boldsymbol{\sigma} \mid \Phi(\boldsymbol{\sigma}, \sigma_y) < 0\}. \tag{6.87}$$

Pressure-insensitivity

Due to its definition exclusively in terms of *shear* stress, the Tresca criterion is *pressure insensitive*, that is, the hydrostatic pressure component,

$$p \equiv \tfrac{1}{3}\,\mathrm{tr}[\boldsymbol{\sigma}] = \tfrac{1}{3}\,(\sigma_1 + \sigma_2 + \sigma_3), \tag{6.88}$$

of the stress tensor does *not* affect yielding. Indeed, note that the superposition of an arbitrary pressure, p^*, on the stress tensor does not affect the value of the Tresca yield function

$$\Phi(\boldsymbol{\sigma} + p^*\boldsymbol{I}) = \Phi(\boldsymbol{\sigma}). \tag{6.89}$$

We remark that the von Mises criterion described in Section 6.4.2 below is also pressure-insensitive. This property is particularly relevant in the modelling of metals as, for these materials, the influence of the hydrostatic stress on yielding is usually negligible in practice.

Isotropy

One very important aspect of the Tresca criterion is its *isotropy* (a property shared by the von Mises, Mohr–Coulomb and Drucker–Prager criteria described in the following sections).

Note that, since Φ in (6.83) or (6.84) is defined as a function of the principal stresses, the Tresca yield function is an *isotropic* function of the stress tensor (refer to Section A.1, page 731, for the definition of isotropic scalar functions of a symmetric tensor), i.e. it satisfies

$$\Phi(\boldsymbol{\sigma}) = \Phi(\boldsymbol{Q}\boldsymbol{\sigma}\boldsymbol{Q}^T) \tag{6.90}$$

for all rotations $\boldsymbol{Q}$; that is, rotations of the state of stress do not affect the value of the yield function.

At this point, it is convenient to introduce the following definition: *A plastic yield criterion is said to be isotropic if it is defined in terms of an isotropic yield function of the stress tensor.*

Graphical representation

Since any isotropic scalar function of a symmetric tensor can be described as a function of the principal values of its argument, it follows that any iso-surface (i.e. any subset of the function domain with fixed function value) of such functions can be graphically represented as a surface in the space of principal values of the argument. This allows, in particular, the yield surface (refer to expression (6.48), page 150) of any isotropic yield criterion to be represented in a particularly simple and useful format as a three-dimensional surface in the space of principal stresses.

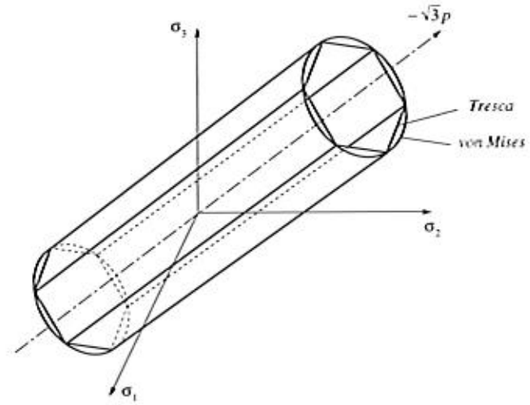

Figure 6.8. The Tresca and von Mises yield surfaces in principal stress space.

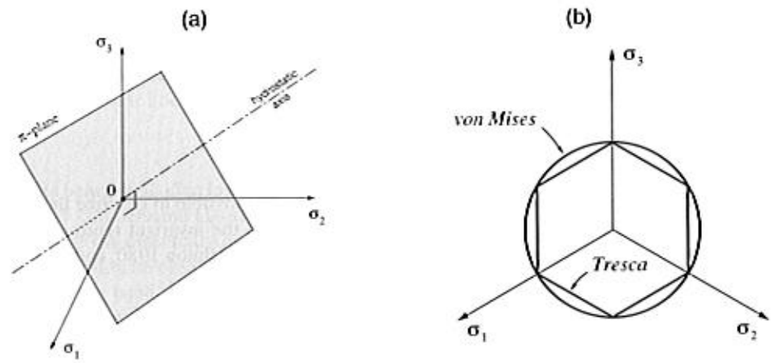

Figure 6.9. (a) The π-plane in principal stress space and, (b) the π-plane representation of the Tresca and von Mises yield surfaces.

In principal stress space, the Tresca yield surface, i.e. the set of stresses for which $\Phi = 0$, is graphically represented by the surface of an infinite hexagonal prism with axis coinciding with the hydrostatic line (also known as the space diagonal), defined by $\sigma_1 = \sigma_2 = \sigma_3$. This is illustrated in Figure 6.8. The elastic domain (for which $\Phi < 0$) corresponds to the interior of the prism. Due to the assumed insensitivity to pressure, a further simplification in the representation of the yield surface is possible in this case. The Tresca yield surface may be represented, without loss of generality, by its projection on the subspace of stresses with zero hydrostatic pressure component ($\sigma_1 + \sigma_2 + \sigma_3 = 0$). This subspace is called the *deviatoric plane*, also referred to as the π-*plane*. It is graphically illustrated in Figure 6.9(a). Figure 6.9(b) shows the π-plane projection of the Tresca yield surface.

Multisurface representation

Equivalently to the above representation, the Tresca yield criterion can be expressed by means of the following six yield functions

$$\begin{aligned}
\Phi_1(\boldsymbol{\sigma}, \sigma_y) &= \sigma_1 - \sigma_3 - \sigma_y \\
\Phi_2(\boldsymbol{\sigma}, \sigma_y) &= \sigma_2 - \sigma_3 - \sigma_y \\
\Phi_3(\boldsymbol{\sigma}, \sigma_y) &= \sigma_2 - \sigma_1 - \sigma_y \\
\Phi_4(\boldsymbol{\sigma}, \sigma_y) &= \sigma_3 - \sigma_1 - \sigma_y \\
\Phi_5(\boldsymbol{\sigma}, \sigma_y) &= \sigma_3 - \sigma_2 - \sigma_y \\
\Phi_6(\boldsymbol{\sigma}, \sigma_y) &= \sigma_1 - \sigma_2 - \sigma_y,
\end{aligned} \tag{6.91}$$

so that, for fixed σ_y, the equation

$$\Phi_i(\boldsymbol{\sigma}, \sigma_y) = 0 \tag{6.92}$$

corresponds to a *plane* in the space of principal stresses for each $i = 1, \ldots, 6$ (Figure 6.10).

In the multisurface representation, the elastic domain for a given σ_y can be defined as

$$\mathcal{E} = \{\boldsymbol{\sigma} \mid \Phi_i(\boldsymbol{\sigma}, \sigma_y) < 0,\ i = 1, \ldots, 6\}. \tag{6.93}$$

Definitions (6.87) and (6.93) are completely equivalent. The yield surface – the boundary of $\mathcal{E}$ – is defined in this case as the set of stresses for which $\Phi_i(\boldsymbol{\sigma}, \sigma_y) = 0$ for at least one i with $\Phi_j(\boldsymbol{\sigma}, \sigma_y) \leq 0$ for $j \neq i$.

Invariant representation

Alternatively to the representations discussed above, it is also possible to describe the yield locus of the Tresca criterion in terms of *stress invariants*. In the invariant representation, proposed by Nayak and Zienkiewicz (1972) (see also Owen and Hinton 1980, and Crisfield 1997), the yield function assumes the format

$$\Phi = 2\sqrt{J_2}\cos\theta - \sigma_y, \tag{6.94}$$

where $J_2 = J_2(\boldsymbol{s})$ is the invariant of the stress deviator, $\boldsymbol{s}$, defined by

$$J_2 \equiv -I_2(\boldsymbol{s}) = \tfrac{1}{2}\,\mathrm{tr}[\boldsymbol{s}^2] = \tfrac{1}{2}\,\boldsymbol{s} : \boldsymbol{s} = \tfrac{1}{2}\,\|\boldsymbol{s}\|^2. \tag{6.95}$$

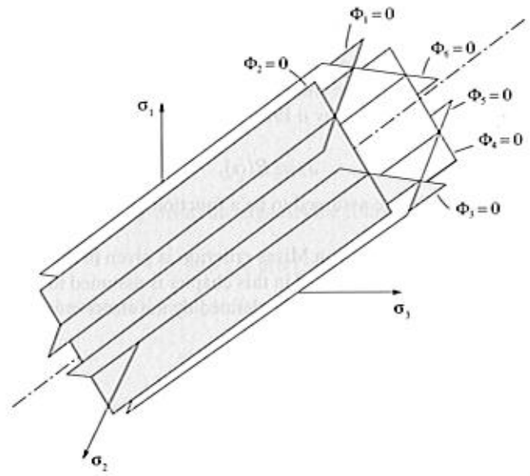

Figure 6.10. The Tresca criterion. Multisurface representation in principal stress space.

Recall that the stress deviator is given by

$$\boldsymbol{s} \equiv \boldsymbol{\sigma} - \tfrac{1}{3}(\mathrm{tr}\boldsymbol{\sigma})\boldsymbol{I}. \tag{6.96}$$

The *Lode angle*, θ, is a function of the deviatoric stress defined as

$$\theta \equiv \tfrac{1}{3}\sin^{-1}\left(\frac{-3\sqrt{3}\,J_3}{2J_2^{\frac{3}{2}}}\right), \tag{6.97}$$

where J_3 is the third principal invariant of stress deviator[5]

$$J_3 \equiv I_3(\boldsymbol{s}) \equiv \det \boldsymbol{s} = \tfrac{1}{3}\,\mathrm{tr}(\boldsymbol{s})^3. \tag{6.98}$$

The Lode angle is the angle, on the deviatoric plane, between $\boldsymbol{s}$ and the nearest pure shear line (a pure shear line is graphically represented in Figure 6.11). It satisfies

$$-\frac{\pi}{6} \leq \theta \leq \frac{\pi}{6}. \tag{6.99}$$

Despite being used often in computational plasticity, the above invariant representation results in rather cumbersome algorithms for integration of the evolution equations of the Tresca model. This is essentially due to the high degree of nonlinearity introduced by the trigonometric function involved in the definition of the Lode angle. The multisurface representation, on the other hand, is found by the authors to provide an optimal parametrisation of the Tresca surface which results in a simpler numerical algorithm and will be adopted in the computational implementation of the model addressed in Chapter 8.

[5] The equivalence between the two rightmost terms in (6.98) is established by summing the characteristic equation (2.73) (page 27) for $i = 1, 2, 3$ and taking into account the fact that $I_1(\boldsymbol{s}) = 0$ ($\boldsymbol{s}$ is a traceless tensor) and that $\mathrm{tr}(\boldsymbol{S})^3 = \sum_i s_i^3$ for any symmetric tensor $\boldsymbol{S}$.

6.4.2. THE VON MISES YIELD CRITERION

Also appropriate to describe plastic yielding in metals, this criterion was proposed by von Mises (1913). According to the von Mises criterion, *plastic yielding begins when the J_2 stress deviator invariant reaches a critical value*. This condition is mathematically represented by the equation

$$J_2 = R(\alpha), \tag{6.100}$$

where R is the critical value, here assumed to be a function of a hardening internal variable, α, to be defined later.

The physical interpretation of the von Mises criterion is given in the following. Since the elastic behaviour of the materials described in this chapter is assumed to be linear elastic, the stored elastic strain-energy at the generic state defined by the stress σ can be decomposed as the sum

$$\psi^e = \psi^e_d + \psi^e_v, \tag{6.101}$$

of a *distortional* contribution,

$$\bar{\rho}\,\psi^e_d = \frac{1}{2\,G}\,\boldsymbol{s} : \boldsymbol{s} = \frac{1}{G}\,J_2, \tag{6.102}$$

and a *volumetric* contribution,

$$\bar{\rho}\,\psi^e_v = \frac{1}{K}\,p^2, \tag{6.103}$$

where G and K are, respectively, the shear and bulk modulus. In view of (6.102), the von Mises criterion is equivalent to stating that *plastic yielding begins when the distortional elastic strain-energy reaches a critical value*. The corresponding critical value of the distortional energy is

$$\frac{1}{G}\,R.$$

It should be noted that, as in the Tresca criterion, the pressure component of the stress tensor does not take part in the definition of the von Mises criterion and only the deviatoric stress can influence plastic yielding. Thus, the von Mises criterion is also *pressure-insensitive*.

In a state of *pure shear*, i.e. a state with stress tensor

$$[\boldsymbol{\sigma}] = \begin{bmatrix} 0 & \tau & 0 \\ \tau & 0 & 0 \\ 0 & 0 & 0 \end{bmatrix}, \tag{6.104}$$

we have, $\boldsymbol{s} = \boldsymbol{\sigma}$ and

$$J_2 = \tau^2. \tag{6.105}$$

Thus, a yield function for the von Mises criterion can be defined as

$$\Phi(\boldsymbol{\sigma}) = \sqrt{J_2(\boldsymbol{s}(\boldsymbol{\sigma}))} - \tau_y, \tag{6.106}$$

where $\tau_y \equiv \sqrt{R}$ is the *shear* yield stress. Let us now consider a state of *uniaxial stress*:

$$[\boldsymbol{\sigma}] = \begin{bmatrix} \sigma & 0 & 0 \\ 0 & 0 & 0 \\ 0 & 0 & 0 \end{bmatrix}. \tag{6.107}$$

In this case, we have

$$[\boldsymbol{s}] = \begin{bmatrix} \frac{2}{3}\sigma & 0 & 0 \\ 0 & -\frac{1}{3}\sigma & 0 \\ 0 & 0 & -\frac{1}{3}\sigma \end{bmatrix} \tag{6.108}$$

and

$$J_2 = \tfrac{1}{3}\sigma^2. \tag{6.109}$$

The above expression for the J_2-invariant suggests the following alternative definition of the von Mises yield function:

$$\Phi(\boldsymbol{\sigma}) = q(\boldsymbol{\sigma}) - \sigma_y, \tag{6.110}$$

where $\sigma_y \equiv \sqrt{3R}$ is the *uniaxial* yield stress and

$$q(\boldsymbol{\sigma}) \equiv \sqrt{3\,J_2(\boldsymbol{s}(\boldsymbol{\sigma}))} \tag{6.111}$$

is termed the *von Mises effective* or *equivalent stress*. The uniaxial and shear yield stresses for the von Mises criterion are related by

$$\sigma_y = \sqrt{3}\,\tau_y. \tag{6.112}$$

Note that this relation differs from that of the Tresca criterion given by (6.85). Obviously, due to its definition in terms of an invariant of the stress tensor, the von Mises yield function is an isotropic function of $\boldsymbol{\sigma}$.

The von Mises and Tresca criteria may be set to agree with one another in either uniaxial stress or pure shear states. If they are set by using the yield functions (6.84) and (6.110) so that both predict the same uniaxial yield stress σ_y, then, under pure shear, the von Mises criterion will predict a yield stress $2/\sqrt{3}$ (≈ 1.155) times that given by the Tresca criterion. On the other hand, if both criteria are made to coincide under pure shear (expressions (6.83) and (6.106) with the same τ_y), then, in uniaxial stress states, the von Mises criterion will predict yielding at a stress level $\sqrt{3}/2$ (≈ 0.866) times the level predicted by Tresca's law.

The yield surface ($\Phi = 0$) associated with the von Mises criterion is represented, in the space of principal stresses, by the surface of an infinite circular cylinder, the axis of which coincides with the hydrostatic axis. The von Mises surface is illustrated in Figure 6.8 where it has been set to match the Tresca surface (shown in the same figure) under uniaxial stress. The corresponding π-plane representation is shown in Figure 6.9(b). The von Mises circle intersects the vertices of the Tresca hexagon. The yield surfaces for the von Mises and Tresca criteria set to coincide in shear is shown in Figure 6.11. In this case, the von Mises circle is tangent to the sides of the Tresca hexagon. It is remarked that, for many metals, experimentally determined yield surfaces fall between the von Mises and Tresca surfaces. A more general model, which includes both the Tresca and the von Mises yield surfaces as particular cases (and, in addition, allows for anisotropy of the yield surface), is described in Section 10.3.4 (starting page 427).

6.4.3. THE MOHR–COULOMB YIELD CRITERION

The criteria presented so far are pressure-insensitive and adequate to describe metals. For materials such as soils, rocks and concrete, whose behaviour is generally characterised by

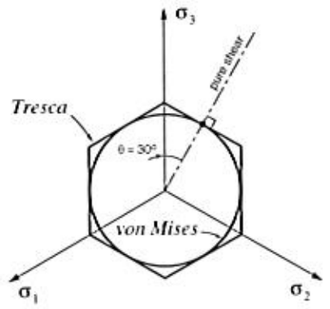

Figure 6.11. Yield surfaces for the Tresca and von Mises criteria coinciding in pure shear.

a strong dependence of the yield limit on the hydrostatic pressure, appropriate description of plastic yielding requires the introduction of *pressure-sensitivity*. A classical example of a pressure-sensitive law is given by the Mohr–Coulomb yield criterion described in the following.

The Mohr–Coulomb criterion is based on the assumption that the phenomenon of macroscopic plastic yielding is, essentially, the result of frictional sliding between material particles. Generalising Coulomb's friction law, this criterion states that *plastic yielding begins when, on a plane in the body, the shearing stress, τ, and the normal stress, σ_n, reach the critical combination*

$$\tau = c - \sigma_n \tan\phi, \tag{6.113}$$

where c is the cohesion and ϕ is the angle of internal friction or frictional angle. In the above, the normal stress, σ_n, was assumed tensile positive.

The yield locus of the Mohr–Coulomb criterion is the set of all stress states such that there exists a plane in which (6.113) holds. The Mohr–Coulomb yield locus can be easily visualised in the Mohr plane representation shown in Figure 6.12. It is the set of all stresses whose largest Mohr circle, i.e. the circle associated with the maximum and minimum principal stresses ($\sigma_{\max}$ and $\sigma_{\min}$, respectively), is tangent to the critical line defined by $\tau = c - \sigma_n \tan\phi$. The elastic domain for the Mohr–Coulomb law is the set of stresses whose all three Mohr circles are below the critical line. From Figure 6.12, the yield condition (6.113) is found to be equivalent to the following form in terms of principal stresses

$$\frac{\sigma_{\max} - \sigma_{\min}}{2}\cos\phi = c - \left(\frac{\sigma_{\max} + \sigma_{\min}}{2} + \frac{\sigma_{\max} - \sigma_{\min}}{2}\sin\phi\right)\tan\phi, \tag{6.114}$$

which, rearranged, gives

$$(\sigma_{\max} - \sigma_{\min}) + (\sigma_{\max} + \sigma_{\min})\sin\phi = 2\,c\,\cos\phi. \tag{6.115}$$

In view of (6.115), a yield function expressed in terms of the principal stresses can be immediately defined for the Mohr–Coulomb criterion as

$$\Phi(\boldsymbol{\sigma}, c) = (\sigma_{\max} - \sigma_{\min}) + (\sigma_{\max} + \sigma_{\min})\,\sin\phi - 2\,c\,\cos\phi. \tag{6.116}$$

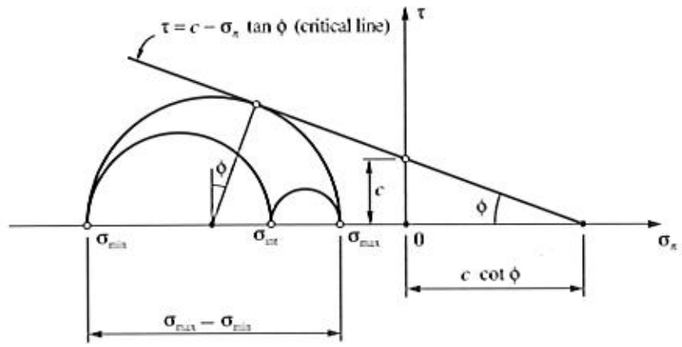

Figure 6.12. The Mohr–Coulomb criterion. Mohr plane representation.

Due to its definition in terms of principal stresses, this yield function is an isotropic function of $\boldsymbol{\sigma}$. The corresponding yield surface ($\Phi = 0$) is a hexagonal pyramid aligned with the hydrostatic axis and whose apex is located at

$$p = c\,\cot\phi \tag{6.117}$$

on the tensile side of the hydrostatic axis. The Mohr–Coulomb surface is illustrated in Figure 6.13. Its pyramidal shape, as opposed to the prismatic shape of the Tresca surface, is a consequence of the *pressure-sensitivity* of the Mohr–Coulomb criterion. It should be noted, however, that both criteria coincide in the absence of internal friction, i.e. when $\phi = 0$. As no stress state is allowed on the outside of the yield surface, the apex of the pyramid (point A in the figure) defines the limit of resistance of the material to tensile pressures. Limited strength under tensile pressure is a typical characteristic of materials such as concrete, rock and soils, to which the Mohr–Coulomb criterion is most applicable.

Multisurface representation

Analogously to the multisurface representation of the Tresca criterion, the Mohr–Coulomb criterion can also be expressed by means of six functions:

$$\begin{aligned}
\Phi_1(\boldsymbol{\sigma}, c) &= \sigma_1 - \sigma_3 + (\sigma_1 + \sigma_3)\sin\phi - 2\,c\,\cos\phi \\
\Phi_2(\boldsymbol{\sigma}, c) &= \sigma_2 - \sigma_3 + (\sigma_2 + \sigma_3)\sin\phi - 2\,c\,\cos\phi \\
\Phi_3(\boldsymbol{\sigma}, c) &= \sigma_2 - \sigma_1 + (\sigma_2 + \sigma_1)\sin\phi - 2\,c\,\cos\phi \\
\Phi_4(\boldsymbol{\sigma}, c) &= \sigma_3 - \sigma_1 + (\sigma_3 + \sigma_1)\sin\phi - 2\,c\,\cos\phi \\
\Phi_5(\boldsymbol{\sigma}, c) &= \sigma_3 - \sigma_2 + (\sigma_3 + \sigma_2)\sin\phi - 2\,c\,\cos\phi \\
\Phi_6(\boldsymbol{\sigma}, c) &= \sigma_1 - \sigma_2 + (\sigma_1 + \sigma_2)\sin\phi - 2\,c\,\cos\phi.
\end{aligned} \tag{6.118}$$

whose roots, $\Phi_i(\boldsymbol{\sigma}, c) = 0$ (for fixed c), define six planes in the principal stress space. Each plane contains one face of the Mohr–Coulomb pyramid represented in Figure 6.13.

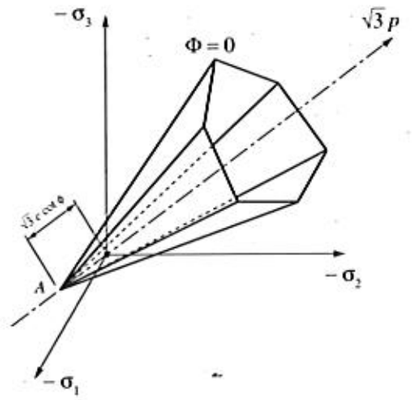

Figure 6.13. The Mohr–Coulomb yield surface in principal stress space.

The definition of the elastic domain and the yield surface in the multisurface representation is completely analogous to that of the Tresca criterion.

Invariant representation

Analogously to the invariant representation (6.94) of the Tresca criterion, the Mohr–Coulomb yield function can be expressed as (Owen and Hinton 1980, and Crisfield 1997):

$$\Phi = \left(\cos\theta - \frac{1}{\sqrt{3}}\sin\theta\,\sin\phi\right)\sqrt{J_2(\boldsymbol{s})} + p(\boldsymbol{\sigma})\,\sin\phi - c\,\cos\phi, \tag{6.119}$$

where the Lode angle, θ, is defined in (6.97). As for the Tresca model, in spite of its frequent use in computational plasticity, the invariant representation of the Mohr–Coulomb surface renders more complex numerical algorithms so that the multisurface representation is preferred in the computational implementation of the model described in Chapter 8.

6.4.4. THE DRUCKER–PRAGER YIELD CRITERION

This criterion has been proposed by Drucker and Prager (1952) as a smooth approximation to the Mohr–Coulomb law. It consists of a modification of the von Mises criterion in which an extra term is included to introduce pressure-sensitivity. The Drucker–Prager criterion states that *plastic yielding begins when the J_2 invariant of the deviatoric stress and the hydrostatic stress, p, reach a critical combination*. The onset of plastic yielding occurs when the equation

$$\sqrt{J_2(\boldsymbol{s})} + \eta\, p = \bar{c}, \tag{6.120}$$

is satisfied, where η and $\bar{c}$ are material parameters. Represented in the principal stress space, the yield locus of this criterion is a circular cone whose axis is the hydrostatic line. For $\eta = 0$, the von Mises cylinder is recovered. The Drucker–Prager cone is illustrated in Figure 6.14.

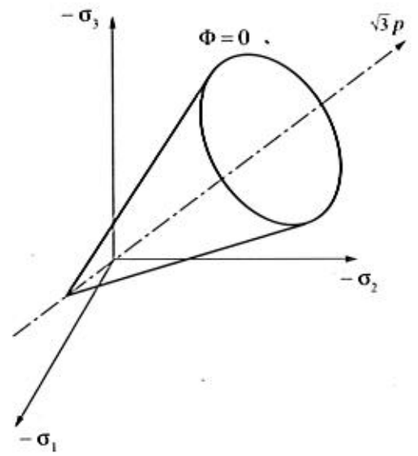

Figure 6.14. The Drucker–Prager yield surface in principal stress space.

In order to approximate the Mohr–Coulomb yield surface, it is convenient to define the Drucker–Prager yield function as

$$\Phi(\boldsymbol{\sigma}, c) = \sqrt{J_2(\boldsymbol{s}(\boldsymbol{\sigma}))} + \eta\, p(\boldsymbol{\sigma}) - \xi\, c, \tag{6.121}$$

where c is the *cohesion* and the parameters η and ξ are chosen according to the required approximation to the Mohr–Coulomb criterion. Note that the isotropy of the Mohr–Coulomb yield function follows from the fact that it is defined in terms of invariants of the stress tensor ($J_2(\boldsymbol{s})$ and p). Two of the most common approximations used are obtained by making the yield surfaces of the Drucker–Prager and Mohr–Coulomb criteria coincident either at the outer or inner edges of the Mohr–Coulomb surface. Coincidence at the *outer* edges is obtained when

$$\eta = \frac{6\,\sin\phi}{\sqrt{3}\,(3 - \sin\phi)}, \quad \xi = \frac{6\,\cos\phi}{\sqrt{3}\,(3 - \sin\phi)}, \tag{6.122}$$

whereas, coincidence at the *inner* edges is given by the choice

$$\eta = \frac{6\,\sin\phi}{\sqrt{3}\,(3 + \sin\phi)}, \quad \xi = \frac{6\,\cos\phi}{\sqrt{3}\,(3 + \sin\phi)}. \tag{6.123}$$

The outer and inner cones are known, respectively, as the *compression cone* and the *extension cone*. The inner cone matches the Mohr–Coulomb criterion in uniaxial tension and biaxial compression. The outer edge approximation matches the Mohr–Coulomb surface in uniaxial compression and biaxial tension. The π-plane section of both surfaces is shown in Figure 6.15. Another popular Drucker–Prager approximation to the Mohr–Coulomb criterion is obtained by forcing both criteria to predict identical collapse loads under *plane strain* conditions. In this case (the reader is referred to Section 4.7 of Chen and Mizuno (1990) for

derivation) the constants η and ξ read

$$\eta = \frac{3\ \tan\phi}{\sqrt{9 + 12\ \tan^2\phi}}, \quad \xi = \frac{3}{\sqrt{9 + 12\ \tan^2\phi}}. \tag{6.124}$$

For all three sets of parameters above, the apex of the approximating Drucker–Prager cone coincides with the apex of the corresponding Mohr–Coulomb yield surface. It should be emphasised here that any of the above approximations to the Mohr–Coulomb criterion can give a poor description of the material behaviour for certain states of stress. Thus, according to the dominant stress state in a particular problem to be analysed, other approximations may be more appropriate. For instance, under plane stress, which can be assumed in the analysis of structures such as concrete walls, it may be convenient to use an approximation such that both criteria match under, say, uniaxial tensile and uniaxial compressive stress states. For the Mohr–Coulomb criterion to fit a given uniaxial tensile strength, f'_t, and a given uniaxial compressive strength, f'_c, the parameters ϕ and c have to be chosen as

$$\phi = \sin^{-1}\left(\frac{f'_c - f'_t}{f'_c + f'_t}\right), \quad c = \frac{f'_c f'_t}{f'_c - f'_t}\tan\phi. \tag{6.125}$$

The corresponding Drucker–Prager cone (Figure 6.16) that predicts the same uniaxial failure loads is obtained by setting

$$\eta = \frac{3\ \sin\phi}{\sqrt{3}}, \quad \xi = \frac{2\cos\phi}{\sqrt{3}}. \tag{6.126}$$

Its apex no longer coincides with the apex of the original Mohr–Coulomb pyramid. For problems where the failure mechanism is indeed dominated by uniaxial tension/compression, the above approximation should produce reasonable results. However, if for a particular problem, failure occurs under biaxial *compression* instead (with stresses near point f'_{bc} of Figure 6.16), then the above approximation will largely overestimate the limit load, particularly for high ratios f'_c/f'_t which are typical for concrete. Under such a condition, a different approximation (such as the inner cone that matches point f'_{bc}) needs to be adopted to produce sensible predictions. Another useful approximation for plane stress, where the Drucker–Prager cone coincides with the Mohr–Coulomb surface in biaxial tension (point f'_{bt}) and biaxial compression (point f'_{bc}), is obtained by setting

$$\eta = \frac{3\ \sin\phi}{2\sqrt{3}}, \quad \xi = \frac{2\cos\phi}{\sqrt{3}}. \tag{6.127}$$

Drucker–Prager approximations to the Mohr–Coulomb criterion are thoroughly discussed by Chen (1982), Chen and Mizuno (1990) and Zienkiewicz *et al.* (1978).

6.5. Plastic flow rules

6.5.1. ASSOCIATIVE AND NON-ASSOCIATIVE PLASTICITY

It has already been said that a plasticity model is classed as *associative* if the yield function, Φ, is taken as the flow potential, i.e.

$$\Psi = \Phi. \tag{6.128}$$

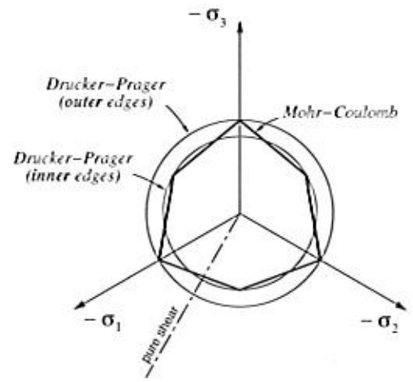

Figure 6.15. The π-plane section of the Mohr–Coulomb surface and the Drucker–Prager approximations.

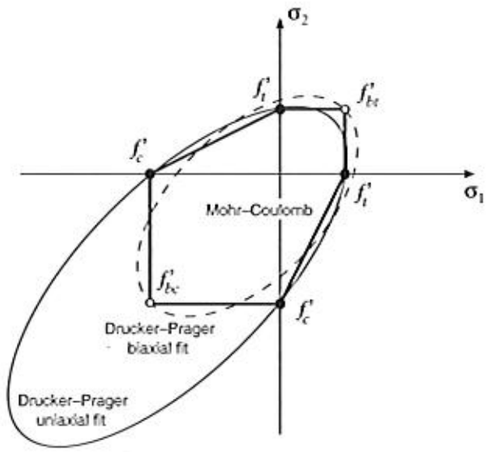

Figure 6.16. Plane stress. Drucker–Prager approximation matching the Mohr–Coulomb surface in uniaxial tension and uniaxial compression.

Any other choice of flow potential characterises a *non-associative* (or *non-associated*) plasticity model.

In associative models, the evolution equations for the plastic strain and hardening variables are given by

$$\dot{\boldsymbol{\varepsilon}}^p = \dot{\gamma}\,\frac{\partial \Phi}{\partial \boldsymbol{\sigma}}, \tag{6.129}$$

and

$$\dot{\boldsymbol{\alpha}} = -\dot{\gamma}\,\frac{\partial \Phi}{\partial \boldsymbol{A}}. \tag{6.130}$$

Associativity implies that the plastic strain rate is a tensor *normal to the yield surface* in the space of stresses. In the generalised case of non-smooth yield surfaces, the flow vector is a subgradient of the yield function, i.e. we have

$$\dot{\boldsymbol{\varepsilon}}^p = \dot{\gamma}\boldsymbol{N}; \quad \boldsymbol{N} \in \partial_{\sigma}\Phi. \tag{6.131}$$

In non-associative models, the plastic strain rate is not normal to the yield surface in general.

6.5.2. ASSOCIATIVE LAWS AND THE PRINCIPLE OF MAXIMUM PLASTIC DISSIPATION

It can be shown that the associative laws are a consequence of the *principle of maximum plastic dissipation*. Before stating the principle of maximum plastic dissipation, recall that for a state defined by a hardening force $\boldsymbol{A}$, the admissible stress states are those that satisfy $\Phi(\boldsymbol{\sigma}, \boldsymbol{A}) \leq 0$. Thus, it makes sense to define

$$\mathscr{A} = \{(\boldsymbol{\sigma}, \boldsymbol{A}) \mid \Phi(\boldsymbol{\sigma}, \boldsymbol{A}) \leq 0\} \tag{6.132}$$

as the set of all admissible pairs (combinations) of stress and hardening force. The principle of maximum dissipation postulates that *among all admissible pairs* $(\boldsymbol{\sigma}^*, \boldsymbol{A}^*) \in \mathscr{A}$, *the actual state* $(\boldsymbol{\sigma}, \boldsymbol{A})$ *maximises the dissipation function* (6.42) *for a given plastic strain rate,* $\dot{\boldsymbol{\varepsilon}}^p$, *and rate* $\dot{\boldsymbol{\alpha}}$ *of hardening internal variables*. The principle of maximum plastic dissipation requires that, for given $(\dot{\boldsymbol{\varepsilon}}^p, \dot{\boldsymbol{\alpha}})$,

$$\Upsilon^p(\boldsymbol{\sigma}, \boldsymbol{A}; \dot{\boldsymbol{\varepsilon}}^p, \dot{\boldsymbol{\alpha}}) \geq \Upsilon^p(\boldsymbol{\sigma}^*, \boldsymbol{A}^*; \dot{\boldsymbol{\varepsilon}}^p, \dot{\boldsymbol{\alpha}}), \ \forall\, (\boldsymbol{\sigma}^*, \boldsymbol{A}^*) \in \mathscr{A}. \tag{6.133}$$

In other words, the actual state $(\boldsymbol{\sigma}, \boldsymbol{A})$ of stress and hardening force is a solution to the following constrained optimisation problem:

$$\begin{aligned} &\text{maximise } \Upsilon^p(\boldsymbol{\sigma}^*, \boldsymbol{A}^*, \dot{\boldsymbol{\varepsilon}}^p, \dot{\boldsymbol{\alpha}}) \\ &\text{subject to } \Phi(\boldsymbol{\sigma}^*, \boldsymbol{A}^*) \leq 0. \end{aligned} \tag{6.134}$$

The *Kuhn–Tucker optimality conditions* (Luenberger, 1973, Chapter 10) for this optimisation problem are precisely the associative plastic flow rule (6.129), the associative hardening rule (6.130) and the loading/unloading conditions

$$\Phi(\boldsymbol{\sigma}, \boldsymbol{A}) \leq 0, \quad \dot{\gamma} \geq 0, \quad \Phi(\boldsymbol{\sigma}, \boldsymbol{A})\dot{\gamma} = 0. \tag{6.135}$$

Remark 6.2. The postulate of maximum plastic dissipation, and the corresponding associative laws, are *not* universal. Based on physical considerations, maximum dissipation has been shown to hold in crystal plasticity and is particularly successful when applied to the description of metals. Nevertheless, for many materials, particularly soils and granular materials in general, associative laws frequently do not correspond to experimental evidence. In such cases, the maximum dissipation postulate is clearly not applicable and the use of non-associative laws is essential.

6.5.3. CLASSICAL FLOW RULES

The Prandtl–Reuss equations

The Prandtl–Reuss plasticity law is the flow rule obtained by taking the von Mises yield function (6.110) as the flow potential. The corresponding flow vector is given by

$$\boldsymbol{N} \equiv \frac{\partial \Phi}{\partial \boldsymbol{\sigma}} = \frac{\partial}{\partial \boldsymbol{\sigma}}[\sqrt{3\,J_2(\boldsymbol{s})}] = \sqrt{\tfrac{3}{2}}\,\frac{\boldsymbol{s}}{||\boldsymbol{s}||}, \tag{6.136}$$

and the flow rule results in

$$\dot{\boldsymbol{\varepsilon}}^p = \dot{\gamma}\,\sqrt{\tfrac{3}{2}}\,\frac{\boldsymbol{s}}{||\boldsymbol{s}||}. \tag{6.137}$$

Here, it should be noted that the Prandtl–Reuss flow vector is the derivative of an isotropic scalar function of a symmetric tensor – the von Mises yield function. Thus (refer to Section A.1.2, page 732, where the derivative of isotropic functions of this type is discussed), $\boldsymbol{N}$ and $\boldsymbol{\sigma}$ are coaxial, i.e. the principal directions of $\boldsymbol{N}$ coincide with those of $\boldsymbol{\sigma}$. Due to the pressure-insensitivity of the von Mises yield function, the plastic flow vector is *deviatoric*. The Prandtl–Reuss flow vector is a tensor parallel to the deviatoric projection $\boldsymbol{s}$ of the stress tensor. Its principal stress representation is depicted in Figure 6.17. The Prandtl–Reuss rule is usually employed in conjunction with the von Mises criterion and the resulting plasticity model is referred to as the von Mises associative model or, simply, the von Mises model.

Associative Tresca

The associative Tresca flow rule utilises the yield function (6.84) as the flow potential. Since Φ here is also an isotropic function of $\boldsymbol{\sigma}$, the rate of plastic strain has the same principal directions as $\boldsymbol{\sigma}$. The Tresca yield function is differentiable when the three principal stresses are distinct ($\sigma_1 \neq \sigma_2 \neq \sigma_3$) and non-differentiable when two principal stresses coincide (at the edges of the Tresca hexagonal prism). Hence, the Tresca associative plastic flow rule is generally expressed as

$$\dot{\boldsymbol{\varepsilon}}^p = \dot{\gamma}\boldsymbol{N}, \tag{6.138}$$

where $\boldsymbol{N}$ is a subgradient of the Tresca function

$$\boldsymbol{N} \in \partial_{\sigma}\Phi. \tag{6.139}$$

Its multisurface-based representation reads

$$\dot{\boldsymbol{\varepsilon}}^p = \sum_{i=1}^{6} \dot{\gamma}^i \boldsymbol{N}^i = \sum_{i=1}^{6} \dot{\gamma}^i \frac{\partial \Phi_i}{\partial \boldsymbol{\sigma}}, \tag{6.140}$$

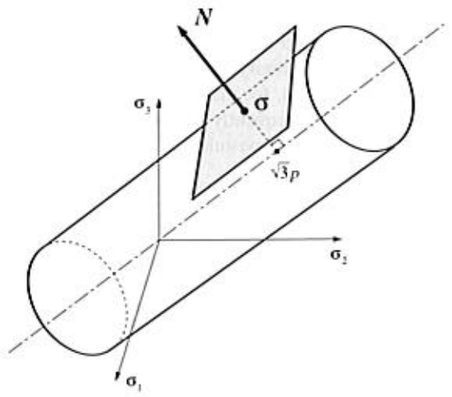

Figure 6.17. The Prandtl–Reuss flow vector.

with the yield functions Φ_i defined by (6.91). Each vector N^i is normal to the plane defined by $\Phi_i = 0$.

The above flow rule can be alternatively expressed as follows. Firstly assume, without loss of generality, that the principal stresses are ordered as $\sigma_1 \geq \sigma_2 \geq \sigma_3$, so that the discussion can be concentrated on the sextant of the π-plane illustrated in Figure 6.18. Three different possibilities have to be considered in this sextant:

(a) yielding at a stress state on the *side* (main plane) of the Tresca hexagon ($\Phi_1 = 0, \Phi_2 < 0$ and $\Phi_6 < 0$);

(b) yielding from the *right corner*, R ($\Phi_1 = 0, \Phi_6 = 0$ and $\Phi_2 < 0$); and

(c) Yielding from the *left corner*, L ($\Phi_1 = 0, \Phi_2 = 0$ and $\Phi_6 < 0$).

When the stress is on the side of the hexagon, only one multiplier may be non-zero and the plastic flow rule reads

$$\dot{\varepsilon}^p = \dot{\gamma}\, N^a, \tag{6.141}$$

where the flow vector is the normal to the plane $\Phi_1 = 0$, given by

$$\begin{aligned} N^a \equiv N^1 &= \frac{\partial \Phi_1}{\partial \boldsymbol{\sigma}} = \frac{\partial}{\partial \boldsymbol{\sigma}}(\sigma_1 - \sigma_3) \\ &= \boldsymbol{e}_1 \otimes \boldsymbol{e}_1 - \boldsymbol{e}_3 \otimes \boldsymbol{e}_3, \end{aligned} \tag{6.142}$$

with $\boldsymbol{e}_i$ denoting the eigenvector of $\boldsymbol{\sigma}$ associated with the principal stress σ_i. In deriving the last right-hand side of (6.142), use has been made of the expression (A.27) of page 736 for the derivative of an eigenvalue of a symmetric tensor.

At the right and left corners of the hexagon, where two planes intersect, two multipliers may be non-zero. Thus, the plastic flow equation is

$$\dot{\varepsilon}^p = \dot{\gamma}^a\, N^a + \dot{\gamma}^b\, N^b. \tag{6.143}$$

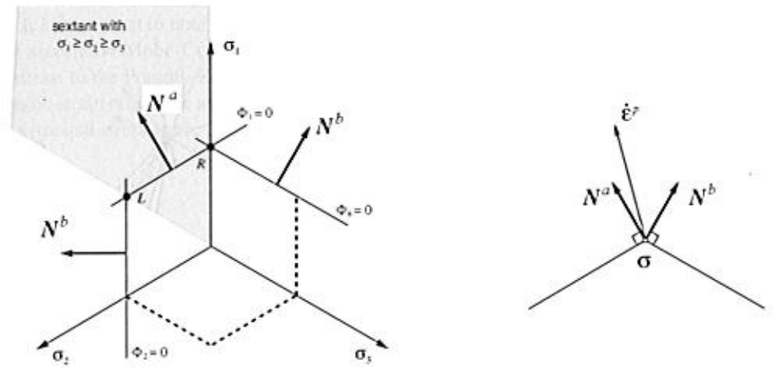

Figure 6.18. The associative Tresca flow rule.

The vector N^a is the normal to the plane $\Phi_1 = 0$, already defined. In the *right corner* (repeated minimum principal stress), the second vector, N^b, is normal to the plane $\Phi_6 = 0$ and is obtained analogously to (6.142) as

$$N^b \equiv N^6 = \boldsymbol{e}_1 \otimes \boldsymbol{e}_1 - \boldsymbol{e}_2 \otimes \boldsymbol{e}_2. \tag{6.144}$$

In the *left corner* (repeated maximum principal stress), N^b, is normal to the plane $\Phi_2 = 0$,

$$N^b \equiv N^2 = \boldsymbol{e}_2 \otimes \boldsymbol{e}_2 - \boldsymbol{e}_3 \otimes \boldsymbol{e}_3. \tag{6.145}$$

It should be noted that, as for the Prandtl–Reuss rule, the plastic flow predicted by the associative Tresca law is *volume-preserving*. Indeed, note that, in the above, we have trivially

$$\operatorname{tr} N^a = \operatorname{tr} N^b = 0. \tag{6.146}$$

This is due to the pressure-insensitivity of the Tresca yield function.

Associative and non-associative Mohr–Coulomb

In the associative Mohr–Coulomb law, the Mohr–Coulomb yield function (6.116) is adopted as the flow potential. Its multisurface representation is based on the yield functions (6.118). The flow rule, which requires consideration of the intersections between the yield surfaces, is derived in a manner analogous to the Tresca law described above. However, it should be noted that in addition to the edge singularities, the present surface has an extra singularity in its apex (Figure 6.13). Plastic yielding may then take place from a face, from an edge or from the apex of the Mohr–Coulomb pyramid.

Again, in the derivation of the flow rules at faces and edges, it is convenient to assume that the principal stresses are ordered as $\sigma_1 \geq \sigma_2 \geq \sigma_3$ so that, without loss of generality, the analysis can be reduced to a single sextant of a cross-section of the Mohr–Coulomb pyramid as illustrated in Figure 6.19. The situation is identical to Tresca's (Figure 6.18) except that

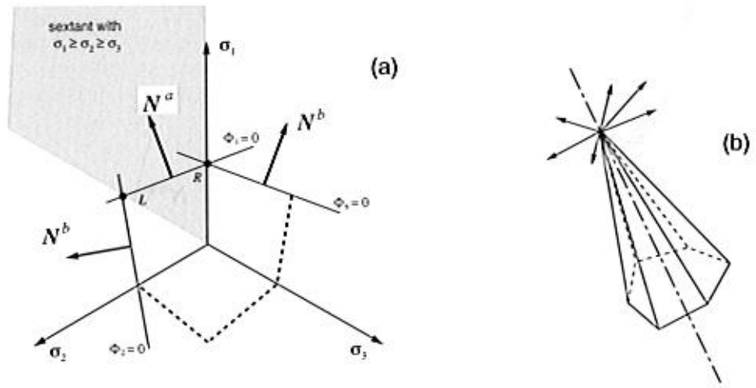

Figure 6.19. The Mohr–Coulomb flow rule; (a) faces and edges, and (b) apex.

the normal vectors N^a and N^b are no longer deviatoric, i.e. they have a non-zero component along the hydrostatic axis (the vectors shown in Figure 6.19 are deviatoric projections of the actual normals). For plastic yielding from the face, the flow rule is given by

$$\dot{\varepsilon}^p = \dot{\gamma}\, N^a, \tag{6.147}$$

where N^a is normal to the plane $\Phi_1 = 0$,

$$\begin{aligned} N^a = \frac{\partial \Phi_1}{\partial \boldsymbol{\sigma}} &= \frac{\partial}{\partial \boldsymbol{\sigma}} \left[\sigma_1 - \sigma_3 + (\sigma_1 + \sigma_3) \sin\phi\right] \\ &= (1 + \sin\phi)\boldsymbol{e}_1 \otimes \boldsymbol{e}_1 - (1 - \sin\phi)\boldsymbol{e}_3 \otimes \boldsymbol{e}_3. \end{aligned} \tag{6.148}$$

At the corners, the above flow rule is replaced by

$$\dot{\varepsilon}^p = \dot{\gamma}^a\, N^a + \dot{\gamma}^b\, N^b. \tag{6.149}$$

At the *right* (extension) corner, R, the second vector, N^b, is normal to the plane $\Phi_6 = 0$ and is given by

$$N^b = (1 + \sin\phi)\, \boldsymbol{e}_1 \otimes \boldsymbol{e}_1 - (1 - \sin\phi)\, \boldsymbol{e}_2 \otimes \boldsymbol{e}_2, \tag{6.150}$$

whereas, at the *left* (compression) corner, L, the tensor N^b is normal to the plane $\Phi_2 = 0$,

$$N^b = (1 + \sin\phi)\, \boldsymbol{e}_2 \otimes \boldsymbol{e}_2 - (1 - \sin\phi)\, \boldsymbol{e}_3 \otimes \boldsymbol{e}_3. \tag{6.151}$$

At the apex of the Mohr–Coulomb surface, all six planes intersect and, therefore, six normals are defined and up to six plastic multipliers may be non-zero. This situation is schematically illustrated in Figure 6.19(b). The plastic strain rate tensor lies within the pyramid defined by the six normals:

$$\dot{\varepsilon}^p = \sum_{i=1}^{6} \dot{\gamma}^i\, N^i. \tag{6.152}$$

It is important to note that, due to the pressure sensitivity of the Mohr–Coulomb criterion, the associative Mohr–Coulomb rule predicts a non-zero *volumetric* plastic straining. This is in contrast to the Prandtl–Reuss and associative Tresca laws. The volumetric component of the plastic strain rate in the associative Mohr–Coulomb law can be obtained by expanding (6.152) in principal stress space taking into account the definitions of N^i. This gives

$$\begin{bmatrix} \dot{\varepsilon}_1^p \\ \dot{\varepsilon}_2^p \\ \dot{\varepsilon}_3^p \end{bmatrix} = \begin{bmatrix} \alpha & 0 & \beta & \beta & 0 & \alpha \\ 0 & \alpha & \alpha & 0 & \beta & \beta \\ \beta & \beta & 0 & \alpha & \alpha & 0 \end{bmatrix} \begin{bmatrix} \dot{\gamma}^1 \\ \dot{\gamma}^2 \\ \dot{\gamma}^3 \\ \dot{\gamma}^4 \\ \dot{\gamma}^5 \\ \dot{\gamma}^6 \end{bmatrix}, \tag{6.153}$$

where

$$\alpha \equiv 1 + \sin\phi, \quad \beta \equiv -1 + \sin\phi. \tag{6.154}$$

The above trivially yields

$$\dot{\varepsilon}_v^p \equiv \dot{\varepsilon}_1^p + \dot{\varepsilon}_2^p + \dot{\varepsilon}_3^p = 2\, \sin\phi \sum_{i=1}^{6} \dot{\gamma}^i. \tag{6.155}$$

As all $\dot{\gamma}^i$'s are non-negative, the volumetric plastic strain rate is positive and, therefore, *dilatant*. The phenomenon of dilatancy during plastic flow is observed for many materials, particularly geomaterials. However, the dilatancy predicted by the associative Mohr–Coulomb law is often excessive. To overcome this problem, it is necessary to use a *non-associated* flow rule in conjunction with the Mohr–Coulomb criterion. The non-associated Mohr–Coulomb law adopts, as flow potential, a Mohr–Coulomb yield function with the frictional angle ϕ replaced by a different (smaller) angle ψ. The angle ψ is called the *dilatancy angle* and the amount of dilation predicted is proportional to its sine. Note that for $\psi = 0$, the plastic flow becomes purely deviatoric and the flow rule reduces to the associative Tresca law.

Associative and non-associative Drucker–Prager

The associative Drucker–Prager model employs as flow potential the yield function defined by (6.121). To derive the corresponding flow rule, one should note first that the Drucker–Prager function is singular at the apex of the yield surface and is smooth anywhere else. Thus, two situations need to be considered:

(a) plastic yielding at (smooth portion of) the cone surface; and

(b) plastic yielding at the apex.

At the cone surface, where the Drucker–Prager yield function is differentiable, the flow vector is obtained by simply differentiating (6.121) which gives (Figure 6.20(a))

$$N = \frac{1}{2\sqrt{J_2(s)}}\, s + \frac{\eta}{3}\, I, \tag{6.156}$$

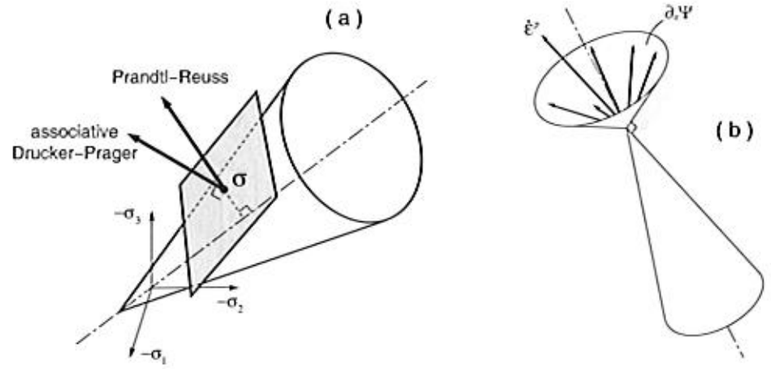

Figure 6.20. The Drucker–Prager flow vector; (a) cone surface, and (b) apex.

where η is given by $(6.122)_1$, $(6.123)_1$ or $(6.124)_1$, according to the chosen approximation to the Mohr–Coulomb surface. The flow rule is then

$$\dot{\varepsilon}^p = \dot{\gamma}\, N. \tag{6.157}$$

The deviatoric/volumetric decomposition of the Drucker–Prager flow vector gives

$$N_d = \frac{1}{2\sqrt{J_2(s)}}\, s, \quad N_v = \eta. \tag{6.158}$$

At the apex singularity, the flow vector is an element of the subdifferential of the yield function (6.121):

$$N \in \partial_\sigma \Phi. \tag{6.159}$$

It lies within the complementary cone to the Drucker–Prager yield surface, i.e. the cone whose wall is normal to the Drucker–Prager cone illustrated in Figure 6.20(b). From standard properties of subdifferentials (Rockafellar, 1970; Rockafellar and Wets, 1998) it can be established that the deviatoric/volumetric split of N in this case is given by

$$N_d \in \partial_\sigma \Phi_d, \quad N_v = \eta, \tag{6.160}$$

where $\Phi_d \equiv \sqrt{J_2(s)}$. Expressions (6.157), (6.158) and (6.160) result in the following rate of (dilatant) volumetric plastic strain for the associative Drucker–Prager flow rule:

$$\dot{\varepsilon}_v^p = \dot{\gamma}\, \eta. \tag{6.161}$$

This expression is analogous to (6.155).

Similarly to the associative Mohr–Coulomb flow rule, the often excessive dilatancy predicted by the associated rule in the present case is avoided by using a non-associated law. The non-associative Drucker–Prager law is obtained by adopting, as the flow potential, a Drucker–Prager yield function with the frictional angle ϕ replaced by a dilatancy angle

$\psi < \phi$; that is, we define

$$\Psi(\boldsymbol{\sigma}, c) = \sqrt{J_2(\boldsymbol{s}(\boldsymbol{\sigma}))} + \bar{\eta}\, p, \tag{6.162}$$

where $\bar{\eta}$ is obtained by replacing ϕ with ψ in the definition of η given by $(6.122)_1$, $(6.123)_1$ or $(6.124)_1$. In other words,

$$\bar{\eta} = \frac{6\,\sin\psi}{\sqrt{3}\,(3-\sin\psi)}, \tag{6.163}$$

when the outer cone approximation to the Mohr–Coulomb criterion is employed. When the inner cone approximation is used,

$$\bar{\eta} = \frac{6\,\sin\psi}{\sqrt{3}\,(3+\sin\psi)}, \tag{6.164}$$

whereas, for the plane strain match,

$$\bar{\eta} = \frac{3\,\tan\psi}{\sqrt{9+12\,\tan^2\psi}}. \tag{6.165}$$

The non-associated Drucker–Prager flow vector differs from its associated counterpart only in the volumetric component which, for the non-associated case, reads

$$N_v = \bar{\eta}. \tag{6.166}$$

If the dilatancy angle of the non-associative potential is chosen as $\psi = 0$, then the volumetric component, N_v, vanishes and the flow rule reduces to the Prandtl–Reuss law that predicts volume-preserving plastic flow (refer to Figure 6.20(a)).

6.6. Hardening laws

The phenomenon of hardening has been identified in the uniaxial experiment described in Section 6.1. Essentially, hardening is characterised by a dependence of yield stress level upon the history of plastic straining to which the body has been subjected. In the uniaxial model, formulated in Section 6.2, this phenomenon has been incorporated by allowing the uniaxial yield stress to vary (as a function of the axial accumulated plastic strain) during plastic flow. In the two- and three-dimensional situations, hardening is represented by changes in the hardening thermodynamical force, A, during plastic yielding. These changes may, in general, affect the size, shape and orientation of the yield surface, defined by $\Phi(\boldsymbol{\sigma}, \boldsymbol{A}) = 0$.

6.6.1. PERFECT PLASTICITY

A material model is said to be *perfectly plastic* if *no hardening* is allowed, that is, the yield stress level does *not* depend in any way on the degree of plastification. In this case, the yield surface remains fixed regardless of any deformation process the material may experience and, in a uniaxial test, the elastoplastic modulus, E^{ep}, vanishes. In the von Mises, Tresca, Drucker–Prager and Mohr–Coulomb models described above, perfect plasticity corresponds to a *constant* uniaxial yield stress, σ_y (or constant cohesion, c). Figure 6.21 shows the stress–strain curve of a typical uniaxial cyclic (tension–compression) test with a perfectly plastic

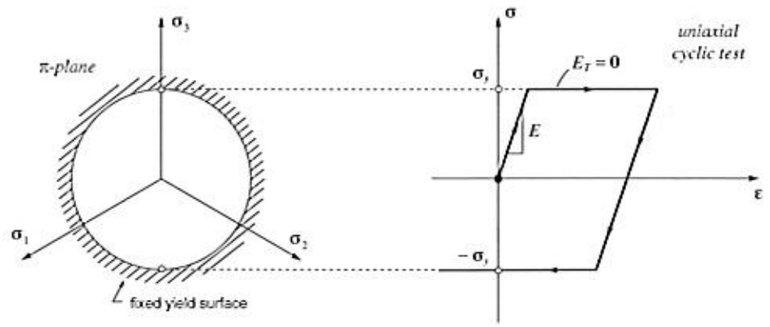

Figure 6.21. Perfect plasticity. Uniaxial test and π-plane representation.

von Mises model along with the corresponding π-plane representation of the yield surface. Perfectly plastic models are particularly suitable for the analysis of the stability of structures and soils and are widely employed in engineering practice for the determination of limit loads and safety factors.

6.6.2. ISOTROPIC HARDENING

A plasticity model is said to be *isotropic hardening* if the evolution of the yield surface is such that, at any state of hardening, it corresponds to a uniform (isotropic) expansion of the initial yield surface, without translation. The uniaxial model described in Section 6.2 is a typical example of an isotropic hardening model. For that model, the elastic domain expands equally in tension and compression during plastic flow. For a multiaxial plasticity model with a von Mises yield surface, isotropic hardening corresponds to the increase in radius of the von Mises cylinder in principal stress space. This, together with a typical stress–strain curve for a uniaxial cyclic test for an isotropic hardening von Mises model is illustrated in Figure 6.22.

The choice of a suitable set (denoted $\boldsymbol{\alpha}$ in Section 6.3) of hardening internal variables must be obviously dependent on the specific characteristics of the material considered. In metal plasticity, for instance, the hardening internal variable is intrinsically connected with the density of dislocations in the crystallographic microstructure that causes an isotropic increase in resistance to plastic flow. In the constitutive description of isotropic hardening, the set $\boldsymbol{\alpha}$ normally contains a single *scalar* variable, which determines the size of the yield surface. Two approaches, *strain hardening* and *work hardening*, are particularly popular in the treatment of isotropic hardening and are suitable for modelling the behaviour of a wide range of materials. These are described below.

Strain hardening

In this case the hardening internal state variable is some suitably chosen scalar measure of *strain*. A typical example is the von Mises *effective plastic strain*, also referred to as the

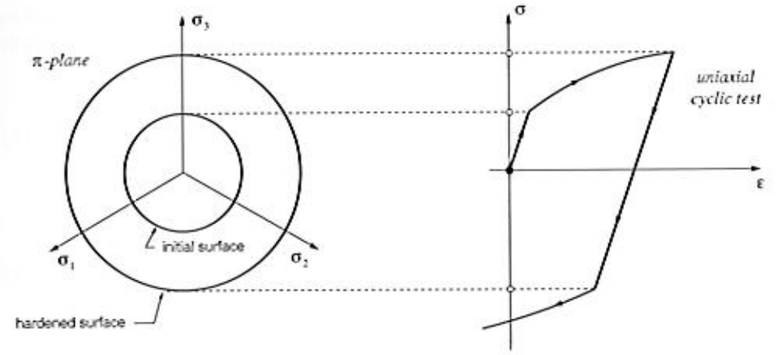

Figure 6.22. Isotropic hardening. Uniaxial test and π-plane representation.

von Mises *equivalent* or *accumulated plastic strain*, defined as

$$\bar{\varepsilon}^p \equiv \int_0^t \sqrt{\tfrac{2}{3}\,\dot{\boldsymbol{\varepsilon}}^p : \dot{\boldsymbol{\varepsilon}}^p}\,\mathrm{d}t = \int_0^t \sqrt{\tfrac{2}{3}}\,\|\dot{\boldsymbol{\varepsilon}}^p\|\,\mathrm{d}t. \tag{6.167}$$

The above definition generalises the accumulated axial plastic strain (6.18) (page 145) of the one-dimensional model to the multiaxially strained case. Its rate evolution equation reads

$$\dot{\bar{\varepsilon}}^p = \sqrt{\tfrac{2}{3}\,\dot{\boldsymbol{\varepsilon}}^p : \dot{\boldsymbol{\varepsilon}}^p} = \sqrt{\tfrac{2}{3}}\,\|\dot{\boldsymbol{\varepsilon}}^p\|, \tag{6.168}$$

or, equivalently, in view of the Prandtl–Reuss flow equation (6.137),

$$\dot{\bar{\varepsilon}}^p = \dot{\gamma}. \tag{6.169}$$

Accordingly, a von Mises isotropic *strain-hardening* model is obtained by letting the uniaxial yield stress be a function of the accumulated plastic strain:

$$\sigma_y = \sigma_y(\bar{\varepsilon}^p). \tag{6.170}$$

This function defines the *strain-hardening curve* (or *strain-hardening function*) that can be obtained, for instance, from a uniaxial tensile test.

Behaviour under uniaxial stress conditions

Under uniaxial stress conditions the von Mises model with isotropic strain hardening reproduces the behaviour of the one-dimensional plasticity model discussed in Section 6.2 and summarised in Box 6.1 (page 146). This is demonstrated in the following. Let us assume that both models share the same Young's modulus, E, and hardening function $\sigma_y = \sigma_y(\bar{\varepsilon}^p)$. Clearly, the two models have identical uniaxial elastic behaviour and initial yield stress. Hence, we only need to show next that their behaviour under plastic yielding is also identical.

Under a uniaxial stress state with axial stress σ and axial stress rate $\dot{\sigma}$ in the direction of the base vector $\boldsymbol{e}_1$, the matrix representations of the stress tensor and the stress rate tensor in the three-dimensional model are given by

$$[\boldsymbol{\sigma}] = \sigma \begin{bmatrix} 1 & 0 & 0 \\ 0 & 0 & 0 \\ 0 & 0 & 0 \end{bmatrix}, \quad [\dot{\boldsymbol{\sigma}}] = \dot{\sigma} \begin{bmatrix} 1 & 0 & 0 \\ 0 & 0 & 0 \\ 0 & 0 & 0 \end{bmatrix}. \tag{6.171}$$

The corresponding stress deviator reads

$$[\boldsymbol{s}] = \tfrac{2}{3}\sigma \begin{bmatrix} 1 & 0 & 0 \\ 0 & -\frac{1}{2} & 0 \\ 0 & 0 & -\frac{1}{2} \end{bmatrix}. \tag{6.172}$$

In this case, the Prandtl–Reuss flow equation (6.137) gives

$$[\dot{\boldsymbol{\varepsilon}}^p] = \dot{\varepsilon}^p \begin{bmatrix} 1 & 0 & 0 \\ 0 & -\frac{1}{2} & 0 \\ 0 & 0 & -\frac{1}{2} \end{bmatrix}, \tag{6.173}$$

where

$$\dot{\varepsilon}^p = \dot{\gamma}\ \mathrm{sign}(\sigma) \tag{6.174}$$

is the axial plastic strain rate. Note that the above expression coincides with the one-dimensional plastic flow rule (6.10). Now, we recall the consistency condition (6.60), which must be satisfied under plastic flow. In the present case, by taking the derivatives of the von Mises yield function (6.110), with σ_y defined by (6.170), we obtain

$$\dot{\Phi} = \boldsymbol{N} : \dot{\boldsymbol{\sigma}} - H\,\dot{\bar{\varepsilon}}^p = 0, \tag{6.175}$$

where $\boldsymbol{N} \equiv \partial\Phi/\partial\boldsymbol{\sigma}$ is the Prandtl–Reuss flow vector (6.136) and $H = H(\bar{\varepsilon}^p)$ is the hardening modulus defined in (6.27). To conclude the demonstration, we combine (6.175) with (6.136), $(6.171)_2$ and (6.172) to recover (6.28) and, then, following the same arguments as in the one-dimensional case we find that, under uniaxial stress conditions, the isotropic strain hardening von Mises model predicts the tangential axial stress–strain relation

$$\dot{\sigma} = \frac{EH}{E+H}\,\dot{\varepsilon}, \tag{6.176}$$

which is identical to equation (6.31) of the one-dimensional model.

Work hardening

In work-hardening models, the variable defining the state of hardening is the dissipated *plastic work*,[¶] w^p, defined by

$$w^p \equiv \int_0^t \boldsymbol{\sigma} : \dot{\boldsymbol{\varepsilon}}^p\, \mathrm{d}t. \tag{6.177}$$

[¶]The term *work hardening* is adopted by many authors as a synonym for the phenomenon of hardening in general. Materials that harden, i.e. materials whose yield stress level depends on the history of strains, are frequently referred to as *work-hardening materials*. In this text, however, the term *work hardening* is reserved for plasticity models in which the dissipated plastic work is taken as the state variable associated with hardening.

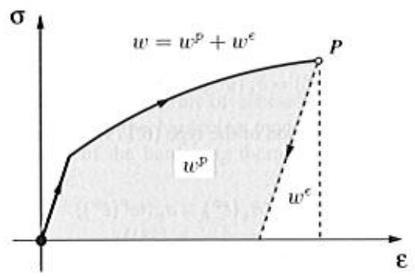

Figure 6.23. The plastic work.

In a uniaxial test, for instance (Figure 6.23), the total work w necessary to deform the material up to point P is given by the total area under the corresponding stress–strain curve. Part of this work, w^e, is stored in the form of elastic energy and is fully recovered upon elastic unloading. The remaining (shaded) area, w^p, is the *plastic work*. It corresponds to the energy dissipated by the plastic mechanisms and cannot be recovered. From the definition of w^p, its evolution equation is given by

$$\dot{w}^p = \boldsymbol{\sigma} : \dot{\boldsymbol{\varepsilon}}^p. \tag{6.178}$$

An isotropic *work-hardening* von Mises model is obtained by postulating

$$\sigma_y = \sigma_y(w^p). \tag{6.179}$$

This defines the *work-hardening curve* (or *work-hardening function*).

Equivalence between strain and work hardening

Under some circumstances, the strain-hardening and work-hardening descriptions are equivalent. This is shown in the following for the von Mises model with associative flow rule (6.137).

The substitution of (6.137) into (6.178), together with the identity $\sqrt{3/2}\|\boldsymbol{s}\| = \sigma_y$ valid for the von Mises model under plastic flow, gives

$$\dot{w}^p = \sigma_y\,\dot{\bar{\varepsilon}}^p, \tag{6.180}$$

or, equivalently,

$$\frac{\mathrm{d}w^p}{\mathrm{d}\bar{\varepsilon}^p} = \sigma_y. \tag{6.181}$$

As σ_y is strictly positive ($\sigma_y > 0$), the above differential relation implies that the mapping between w^p and $\bar{\varepsilon}^p$ is one-to-one and, therefore, invertible so that

$$w^p = w^p(\bar{\varepsilon}^p) \tag{6.182}$$

and

$$\bar{\varepsilon}^p = \bar{\varepsilon}^p(w^p). \tag{6.183}$$

This allows any given strain-hardening function of the type (6.170) to be expressed as an equivalent work-hardening function,

$$\sigma_y(\bar{\varepsilon}^p) = \tilde{\sigma}_y(w^p) \equiv \sigma_y(\bar{\varepsilon}^p(w^p)), \tag{6.184}$$

and any given work-hardening function of the type (6.179) to be expressed as an equivalent strain-hardening function,

$$\sigma_y(w^p) = \hat{\sigma}_y(\bar{\varepsilon}^p) \equiv \sigma_y(w^p(\bar{\varepsilon}^p)). \tag{6.185}$$

Expressions (6.184) and (6.185) establish the equivalence between the strain and work-hardening descriptions for the von Mises model with associative flow rule.

Linear and nonlinear hardening

A model is said to be *linear hardening* if the strain-hardening function (6.170) is linear, i.e. if it can be expressed as

$$\sigma_y(\bar{\varepsilon}^p) = \sigma_{y0} + H\bar{\varepsilon}^p, \tag{6.186}$$

with *constant* σ_{y0} and H. The constant σ_{y0} is the *initial yield stress*, i.e. the uniaxial yield stress at the initial (*virgin*) state of the material, and H is called the *linear isotropic hardening modulus*. Any other hardening model is said to be *nonlinear hardening*. Note that perfect plasticity (defined in Section 6.6.1) is obtained if we set $H = 0$ in (6.186).

It should also be noted that a linear *work*-hardening function corresponds in general to an equivalent *nonlinear* strain-hardening function (i.e. a nonlinear hardening model). This can be easily established by observing that (6.181) defines a nonlinear relation between w^p and $\bar{\varepsilon}^p$ if σ_y is not a constant.

6.6.3. THERMODYNAMICAL ASPECTS. ASSOCIATIVE ISOTROPIC HARDENING

Within the formalism of thermodynamics with internal variables, the above isotropic strain-hardening law corresponds to the assumption that the plastic contribution, ψ^p, to the free energy (recall expression (6.37), page 149) is a function of a single scalar argument – the accumulated plastic strain. That is, the set $\boldsymbol{\alpha}$ of hardening variables is defined as

$$\boldsymbol{\alpha} \equiv \{\bar{\varepsilon}^p\} \tag{6.187}$$

and

$$\psi^p = \psi^p(\bar{\varepsilon}^p). \tag{6.188}$$

The set of hardening thermodynamic forces in this case specialises as

$$\boldsymbol{A} \equiv \{\kappa\}, \tag{6.189}$$

where the scalar thermodynamic force, κ, associated to isotropic hardening is defined by

$$\kappa \equiv \bar{\rho}\frac{\partial \psi^p}{\partial \bar{\varepsilon}^p} = \kappa(\bar{\varepsilon}^p). \tag{6.190}$$

The hardening curve is postulated in terms of κ as

$$\sigma_y(\bar{\varepsilon}^p) \equiv \sigma_{y0} + \kappa(\bar{\varepsilon}^p). \tag{6.191}$$

If the state of hardening is defined in terms of cohesion (or shear yield stress), c (or τ_y) replaces σ_y in (6.191). Note that the hardening modulus H, initially defined in (6.27), represents the rate of change of the hardening thermodynamic force with respect to the hardening internal variable, i.e.

$$H(\bar{\varepsilon}^p) \equiv \frac{\partial \sigma_y}{\partial \bar{\varepsilon}^p} = \frac{\partial \kappa}{\partial \bar{\varepsilon}^p}. \tag{6.192}$$

For the strain-hardening von Mises model the evolution law (6.168) and (6.169) for the internal variable, $\bar{\varepsilon}^p$, follows from the hypothesis of *associativity*, that relies on the choice of the yield function as the plastic potential. The associative evolution equation for $\bar{\varepsilon}^p$ in this case is a specialisation of (6.130); that is, we have

$$\dot{\bar{\varepsilon}}^p = \dot{\gamma}\boldsymbol{H} = \dot{\gamma}. \tag{6.193}$$

The associative generalised modulus $\boldsymbol{H}$ is given by

$$\boldsymbol{H} = -\frac{\partial \Phi}{\partial \boldsymbol{A}} \equiv -\frac{\partial \Phi}{\partial \kappa} = 1, \tag{6.194}$$

where Φ is the von Mises yield function (6.110). A hardening law defined by means of the associativity hypothesis is called an *associative hardening* law. Any other hardening rule is said to be *non-associative*.

Multisurface models with associative hardening

Analogously to the associative plastic flow rule definition (6.73), (6.77) and (6.78), associative hardening for multisurface plasticity models can be defined by postulating the following generic evolution equation for the accumulated plastic strain:

$$\dot{\bar{\varepsilon}}^p = -\sum_{i=1}^{n} \dot{\gamma}^i \frac{\partial \Phi_i}{\partial \kappa}. \tag{6.195}$$

Note that, here, the accumulated plastic strain, $\bar{\varepsilon}^p$, is being *defined* by evolution equation (6.195). Its actual physical meaning depends on the specific format of the functions Φ_i and is generally different from that of (6.167) adopted for the von Mises model.

A simple example of associative isotropic hardening law of the type (6.195) is obtained for the Tresca model. Here, we refer to the plastic flow equations (6.141) and (6.143), defined respectively on the side (smooth portion) and corner of the Tresca yield surface. The corresponding associative evolution equations that define the accumulated plastic strain $\bar{\varepsilon}^p$ are

$$\dot{\bar{\varepsilon}}^p = -\dot{\gamma}\frac{\partial \Phi_1}{\partial \kappa} = \dot{\gamma} \tag{6.196}$$

and

$$\dot{\bar{\varepsilon}}^p = -\dot{\gamma}^a \frac{\partial \Phi_1}{\partial \kappa} - \dot{\gamma}^b \frac{\partial \Phi_6}{\partial \kappa} = \dot{\gamma}^a + \dot{\gamma}^b, \tag{6.197}$$

respectively, where functions Φ_1 and Φ_6 are defined by (6.91) with σ_y related to κ through (6.191).

For Mohr–Coulomb plasticity, one of the possibilities in defining a hardening law is to assume the *cohesion*, c, that takes part of the yield function (6.116) or (6.121) to be a function of the hardening internal variable:

$$c = c(\bar{\varepsilon}^p). \tag{6.198}$$

This type of hardening description is often used in practice in the modelling of soils – for which cohesion is a fundamental strength parameter. This assumption will be adopted in the computer implementation of Mohr–Coulomb and Drucker–Prager models described in Chapter 8. If hardening associativity is also assumed, then similarly to (6.191) we define

$$c(\bar{\varepsilon}^p) = c_0 + \kappa(\bar{\varepsilon}^p), \tag{6.199}$$

and the internal variable $\bar{\varepsilon}^p$ – the accumulated plastic strain for associative Mohr–Coulomb hardening – is defined by the corresponding particularisation of general evolution law (6.195). This gives the general expression

$$\dot{\bar{\varepsilon}}^p = 2\cos\phi \sum_{i=1}^{6} \dot{\gamma}^i. \tag{6.200}$$

When flow takes place at the smooth portion of a Mohr–Coulomb pyramid face, this is reduced to

$$\dot{\bar{\varepsilon}}^p = 2\cos\phi\,\dot{\gamma}. \tag{6.201}$$

At the corners (refer to the plastic flow equation (6.149)), we have

$$\dot{\bar{\varepsilon}}^p = 2\cos\phi\,(\dot{\gamma}^a + \dot{\gamma}^b). \tag{6.202}$$

Note that if it is insisted to adopt the von Mises accumulated plastic strain rate definition (6.167) in conjunction, say, with the Tresca model with associative plastic flow, (6.141) to (6.143), the evolution equation for $\bar{\varepsilon}^p$ will result in

$$\dot{\bar{\varepsilon}}^p = \sqrt{\tfrac{2}{3}\,\dot{\boldsymbol{\varepsilon}}^p : \dot{\boldsymbol{\varepsilon}}^p} = \tfrac{2}{\sqrt{3}}\,\dot{\gamma} \tag{6.203}$$

for flow from the smooth portions of the Tresca surface, and

$$\dot{\bar{\varepsilon}}^p = \sqrt{\tfrac{2}{3}\,\dot{\boldsymbol{\varepsilon}}^p : \dot{\boldsymbol{\varepsilon}}^p} = \tfrac{2}{\sqrt{3}}\,\sqrt{(\dot{\gamma}^a)^2 + \dot{\gamma}^a\dot{\gamma}^b + (\dot{\gamma}^b)^2}, \tag{6.204}$$

for flow from a corner. In this case, the isotropic hardening law is *non-associative* in spite of the associativity of the plastic flow rule.

Drucker–Prager associative hardening

Associative hardening for Drucker–Prager plasticity is obtained by combining assumption (6.199) and the yield function definition (6.121) with the general associative evolution law (6.130) for the hardening internal variable. The accumulated plastic strain in this case is then defined by the evolution equation

$$\dot{\bar{\varepsilon}}^p = -\dot{\gamma}\,\frac{\partial \Phi}{\partial \kappa} = \dot{\gamma}\,\xi. \tag{6.205}$$

Other hardening models

Further refinements to capture hardening behaviour more accurately can be incorporated in Mohr–Coulomb based plasticity models by assuming, in addition, the frictional angle to be a function, for example, of the accumulated plastic strain:

$$\phi = \phi(\bar{\varepsilon}^p). \tag{6.206}$$

For Drucker–Prager-based models, the above would correspond to having

$$\eta = \eta(\bar{\varepsilon}^p), \quad \xi = \xi(\bar{\varepsilon}^p). \tag{6.207}$$

The direction of plastic flow is generally affected by the history of plastic straining in materials such as soils and rocks. This phenomenon can be accounted for in non-associative flow Mohr–Coulomb type models by letting the dilatancy angle, ψ, be a function of the hardening internal variable. For Drucker–Prager-based models, this can be obtained by having the parameter $\bar{\eta}$ as a function of the hardening variable.

6.6.4. KINEMATIC HARDENING. THE BAUSCHINGER EFFECT

When the yield surfaces preserve their shape and size but *translate* in the stress space as a rigid body, *kinematic hardening* is said to take place. It is frequently observed in experiments that, after being loaded (and hardened) in one direction, many materials show a decreased resistance to plastic yielding in the opposite direction (Lemaitre and Chaboche, 1990). This phenomenon is known as the *Bauschinger effect* and can be modelled with the introduction of kinematic hardening. A number of constitutive models have been proposed to describe elastoplastic behaviour under cyclic loading conditions (Lemaitre and Chaboche, 1990; Mróz, 1967; Skrzypek, 1993). The typical result of a uniaxial cyclic test showing the Bauschinger effect is illustrated in Figure 6.24. The evolution of a kinematically hardening von Mises-type yield surface (in the deviatoric plane) used to model the phenomenon is shown alongside. The yield function for the kinematically hardening model is given by

$$\Phi(\boldsymbol{\sigma}, \boldsymbol{\beta}) = \sqrt{3\,J_2(\boldsymbol{\eta}(\boldsymbol{\sigma}, \boldsymbol{\beta}))} - \sigma_y, \tag{6.208}$$

where

$$\boldsymbol{\eta}(\boldsymbol{\sigma}, \boldsymbol{\beta}) \equiv \boldsymbol{s}(\boldsymbol{\sigma}) - \boldsymbol{\beta} \tag{6.209}$$

is the *relative stress* tensor, defined as the difference between the stress deviator and the symmetric deviatoric (stress-like) tensor, $\boldsymbol{\beta}$, known as the *back-stress* tensor. Note that, by definition, the relative stress is *deviatoric*. The back-stress tensor is the thermodynamical force associated with kinematic hardening and represents the translation (Figure 6.24) of the yield surface in the space of stresses. The *constant* σ_y in (6.208) defines the radius of the yield surface. When $\boldsymbol{\beta} = \mathbf{0}$, we have $\boldsymbol{\eta} = \boldsymbol{s}$ and the yield surface defined by $\Phi = 0$ is the isotropic von Mises yield surface with uniaxial yield stress σ_y.

It is important to observe that, unlike the isotropically hardening von Mises model, the yield function Φ defined by (6.208) is *not* an isotropic function of the stress tensor for kinematically hardened states ($\boldsymbol{\beta} \neq \mathbf{0}$). The function (6.208) is an isotropic function of the *relative stress*, $\boldsymbol{\eta}$. Analogously to expression (6.208), it is possible to introduce kinematic hardening in other plasticity models simply by replacing $\boldsymbol{\sigma}$ with a relative stress measure, defined as the difference $\boldsymbol{\sigma} - \boldsymbol{\beta}$, in the definition of the corresponding yield function.

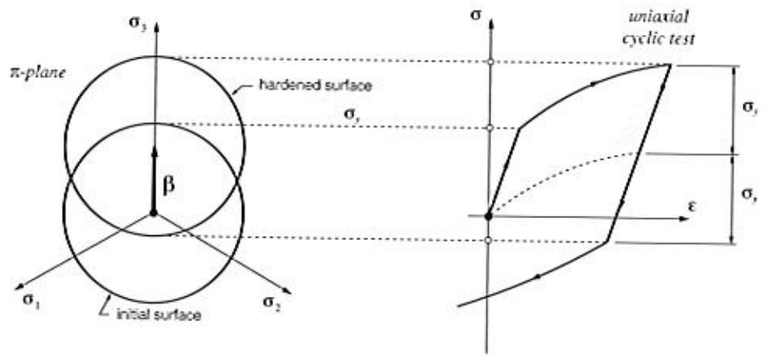

Figure 6.24. Kinematic hardening and the *Bauschinger effect*. Uniaxial test and π-plane representation. Loading in one direction results in decreased resistance to plastic yielding in the opposite direction.

Plastic flow rule with kinematic hardening

The von Mises model with kinematic hardening is used in conjunction with an *associative* flow rule. The flow vector in this case reads

$$N \equiv \frac{\partial \Phi}{\partial \boldsymbol{\sigma}} = \sqrt{\tfrac{3}{2}} \frac{\boldsymbol{\eta}}{\|\boldsymbol{\eta}\|} \tag{6.210}$$

and we have the following plastic strain rate equation:

$$\dot{\boldsymbol{\varepsilon}}^P = \dot{\gamma}\, N = \dot{\gamma} \sqrt{\tfrac{3}{2}} \frac{\boldsymbol{\eta}}{\|\boldsymbol{\eta}\|}. \tag{6.211}$$

This rule extends the Prandtl–Reuss equation to account for kinematic hardening. Note that the plastic flow is in the direction of the (deviatoric) relative stress, $\boldsymbol{\eta}$, and coincides with the Prandtl–Reuss equation if $\boldsymbol{\beta} = \mathbf{0}$.

Prager's linear kinematic hardening

To complete the definition of the kinematic hardening plasticity model, evolution equations for $\boldsymbol{\beta}$ are required. One of the most commonly used laws is *Prager's linear kinematic hardening rule*, where the rate evolution equation for $\boldsymbol{\beta}$ is given by

$$\dot{\boldsymbol{\beta}} = \tfrac{2}{3} H\, \dot{\boldsymbol{\varepsilon}}^P = \dot{\gamma} \sqrt{\tfrac{2}{3}}\, H \frac{\boldsymbol{\eta}}{\|\boldsymbol{\eta}\|}. \tag{6.212}$$

The material constant H is the *linear kinematic hardening modulus*.

Behaviour under monotonic uniaxial stress loading

For monotonic loading under uniaxial stress conditions, the stress–strain behaviour of the model defined by equations (6.208), with constant $\sigma_y = \sigma_{y0}$, (6.211) and (6.212) and initial

state of hardening defined by $\boldsymbol{\beta} = \mathbf{0}$ is identical to the behaviour of the purely isotropic hardening von Mises model with linear hardening curve (6.186) and initial state of hardening $\bar{\varepsilon}^P = 0$. It is assumed in this statement that both models share the same Young's modulus, E. Under the above conditions, it is clear that both models have the same elastic behaviour and uniaxial yield stress, σ_{y0}. To show that their plastic behaviour also coincides, let us consider again a uniaxial test with loading in the direction of the base vector $\boldsymbol{e}_1$. In this case, the stress, stress rate and stress deviator tensors have the matrix representations given in (6.171) and (6.172). Now note that the integration of the rate equation (6.212) with initial condition $\boldsymbol{\beta} = \mathbf{0}$ (i.e. $\boldsymbol{\eta} = \boldsymbol{s}$) and $\boldsymbol{s}$ as in (6.172) gives a back-stress tensor of the form

$$[\boldsymbol{\beta}] = \beta \begin{bmatrix} 1 & 0 & 0 \\ 0 & -\frac{1}{2} & 0 \\ 0 & 0 & -\frac{1}{2} \end{bmatrix}, \tag{6.213}$$

where β is the axial back-stress component. With the above, we obtain for the relative stress tensor

$$[\boldsymbol{\eta}] = \eta \begin{bmatrix} 1 & 0 & 0 \\ 0 & -\frac{1}{2} & 0 \\ 0 & 0 & -\frac{1}{2} \end{bmatrix}, \tag{6.214}$$

where

$$\eta = \tfrac{2}{3}\sigma - \beta \tag{6.215}$$

is the axial relative stress. From (6.212) and (6.214) we obtain

$$[\dot{\boldsymbol{\beta}}] = \tfrac{2}{3} H \dot{\varepsilon}^P \begin{bmatrix} 1 & 0 & 0 \\ 0 & -\frac{1}{2} & 0 \\ 0 & 0 & -\frac{1}{2} \end{bmatrix}, \tag{6.216}$$

where $\dot{\varepsilon}^P$ is the axial plastic strain rate given by

$$\dot{\varepsilon}^P = \dot{\gamma}\, \mathrm{sign}(\eta). \tag{6.217}$$

Now, by recalling (6.60) and specialising (6.61) for the present case we have that, under plastic yielding, the following consistency condition must be satisfied:

$$\dot{\Phi} = \frac{\partial \Phi}{\partial \boldsymbol{\sigma}} : \dot{\boldsymbol{\sigma}} + \frac{\partial \Phi}{\partial \boldsymbol{\beta}} : \dot{\boldsymbol{\beta}} = 0. \tag{6.218}$$

After some straightforward tensor algebra, taking into account $(6.171)_2$ and the above expressions for $\dot{\boldsymbol{\beta}}$, $\boldsymbol{\beta}$, the definition of $\boldsymbol{\eta}$, and the identity

$$\frac{\partial \Phi}{\partial \boldsymbol{\beta}} = -\frac{\partial \Phi}{\partial \boldsymbol{\sigma}} = -\sqrt{\frac{3}{2}} \frac{\boldsymbol{\eta}}{\|\boldsymbol{\eta}\|}, \tag{6.219}$$

equation (6.218) yields

$$\dot{\sigma} = H \dot{\varepsilon}^P. \tag{6.220}$$

Then, with the introduction of the elastoplastic split of the axial strain rate, together with the equation

$$\dot{\sigma} = E \dot{\varepsilon}^e, \tag{6.221}$$

of the linear elastic model under uniaxial stress conditions, into (6.220), we obtain

$$\dot{\sigma} = \frac{EH}{E+H}\,\dot{\varepsilon}, \tag{6.222}$$

which coincides with the stress rate equation (6.176) of the von Mises isotropic strain-hardening model with constant H. To complete the demonstration, let us assume that the uniaxial loading is monotonic, i.e. we have either $\dot{\varepsilon} > 0$ or $\dot{\varepsilon} < 0$ throughout the entire loading process. In this case, the integration of (6.222) having the initial yield stress (σ_{y0} for both models) as the initial condition produces the same stress–strain curve as the isotropic model.

Armstrong–Frederick hardening

A refinement upon the linear kinematic hardening law proposed by Armstrong and Frederick (1966) is obtained by introducing an extra term in the above expression (refer to Lemaitre and Chaboche (1990), Chapter 5, or Jirásek and Bažant (2002), Chapter 20, for details) with the evolution of $\boldsymbol{\beta}$ given by

$$\begin{aligned}\dot{\boldsymbol{\beta}} &= \frac{2}{3}\,H\,\dot{\boldsymbol{\varepsilon}}^p - \dot{\gamma}\,b\,\boldsymbol{\beta} \\ &= \dot{\gamma}\left(\frac{2}{3}H\,\frac{\partial\Phi}{\partial\boldsymbol{\sigma}} - b\,\boldsymbol{\beta}\right),\end{aligned} \tag{6.223}$$

where b is a material constant. The extra term $-\dot{\gamma}\,b\,\boldsymbol{\beta}$ introduces the effect of saturation in the kinematic hardening rule. In the case of the von Mises criterion, the saturation corresponds to a maximum limit value for the norm of $\boldsymbol{\beta}$, at which the material behaves as perfectly plastic.

Nonlinear extension to Prager's rule

Another possible improvement upon Prager's linear kinematic hardening rule is the introduction of nonlinearity by replacing the constant kinematic hardening modulus, H, of (6.212) with a generic function of the accumulated plastic strain, $\bar{\varepsilon}^p$,

$$\dot{\boldsymbol{\beta}} = \frac{2}{3}H(\bar{\varepsilon}^p)\,\dot{\boldsymbol{\varepsilon}}^p = \dot{\gamma}\,\frac{2}{3}H(\bar{\varepsilon}^p)\,\frac{\partial\Phi}{\partial\boldsymbol{\sigma}}. \tag{6.224}$$

In this case, a scalar function

$$\bar{\beta} \equiv \bar{\beta}(\bar{\varepsilon}^p), \tag{6.225}$$

such that

$$H(\bar{\varepsilon}^p) = \frac{\mathrm{d}\bar{\beta}}{\mathrm{d}\bar{\varepsilon}^p}, \tag{6.226}$$

defines the *kinematic hardening curve*. This curve can be obtained from simple uniaxial tests in a manner analogous to the determination of the hardening curve for the purely isotropic hardening model.

Thermodynamical aspects of kinematic hardening

From the thermodynamical viewpoint, the above kinematic hardening laws follow from the assumption that the plastic contribution, ψ^p, to the free energy is a function of a second-order tensor-valued internal variable, $\boldsymbol{X}$,

$$\psi^p = \psi^p(\boldsymbol{X}). \tag{6.227}$$

The variable $\boldsymbol{X}$ is related to self-equilibrated residual stresses that remain after elastic unloading. These stresses may increase or decrease resistance to plastic slip according to the direction considered. The kinematic hardening thermodynamical force – the back-stress tensor, $\boldsymbol{\beta}$ – is then defined as the derivative

$$\boldsymbol{\beta} \equiv \frac{\partial\psi^p}{\partial\boldsymbol{X}}. \tag{6.228}$$

For the Armstrong–Frederick kinematic hardening law (6.223), for instance, we have

$$\psi^p(\boldsymbol{X}) = \frac{a}{2}\,\boldsymbol{X} : \boldsymbol{X}, \tag{6.229}$$

where the material constant a has been defined as

$$a \equiv \tfrac{2}{3}\,H. \tag{6.230}$$

The back-stress tensor (6.228) is then a scalar multiple of $\boldsymbol{X}$, given by

$$\boldsymbol{\beta} = a\,\boldsymbol{X}. \tag{6.231}$$

The evolution law for the internal variable $\boldsymbol{X}$ is obtained by postulating a flow potential

$$\Psi \equiv \Phi + \frac{b}{2a}\boldsymbol{\beta} : \boldsymbol{\beta}, \tag{6.232}$$

and assuming normal dissipativity

$$\dot{\boldsymbol{X}} \equiv -\dot{\gamma}\,\frac{\partial\Psi}{\partial\boldsymbol{\beta}} = -\dot{\gamma}\left(\frac{\partial\Phi}{\partial\boldsymbol{\beta}} + \frac{b}{a}\,\boldsymbol{\beta}\right). \tag{6.233}$$

Obviously (since $\Psi \neq \Phi$), this evolution law is *non-associative*. The equivalence between the above equation and (6.223) can be established by taking into account (6.231) and the fact that, since Φ is obtained from a non-kinematic hardening yield function by replacing the argument $\boldsymbol{\sigma}$ with $\boldsymbol{\sigma} - \boldsymbol{\beta}$, we have

$$\frac{\partial\Phi}{\partial\boldsymbol{\beta}} = -\frac{\partial\Phi}{\partial\boldsymbol{\sigma}}. \tag{6.234}$$

6.6.5. MIXED ISOTROPIC/KINEMATIC HARDENING

Rather than purely isotropic or purely kinematic hardening, real-life materials show in general a combination of both; that is, under plastic straining, the yield surface expands/shrinks and translates simultaneously in stress space. Thus, more realistic plasticity models can be obtained by combining the above laws for isotropic and kinematic hardening.

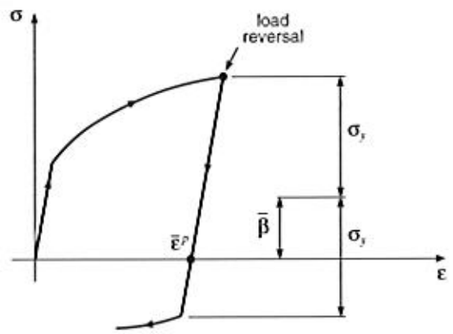

Figure 6.25. Mixed hardening. Uniaxial test with load reversal.

For example, a relatively simple von Mises-based model with mixed isotropic/kinematic hardening can be devised by adopting the yield function (6.208) and allowing σ_y to be a function of $\bar{\varepsilon}^p$. If the nonlinear rule defined by (6.224) and (6.225) is adopted, the hardening behaviour of the model is determined by the curves

$$\sigma_y = \sigma_y(\bar{\varepsilon}^p), \quad \bar{\beta} = \bar{\beta}(\bar{\varepsilon}^p), \tag{6.235}$$

which can be obtained from relatively simple uniaxial tests with load reversal (see schematic illustration of Figure 6.25). At each point $\bar{\varepsilon}^p$, the *kinematic hardening stress*, $\bar{\beta}$, is the kinematic contribution to overall hardening.

A more refined mixed hardening model can be devised by coupling the Armstrong–Frederick law (6.223) with the von Mises-type yield function (6.208) where σ_y, as in $(6.235)_1$, is a function of the accumulated plastic strain. A model including mixed hardening of this type is discussed in Section 12.3 (starting on page 478) in the context of damage mechanics.

7 FINITE ELEMENTS IN SMALL-STRAIN PLASTICITY PROBLEMS

IN the previous chapter, the mathematical theory of plasticity has been reviewed. A general small-strain elastoplastic constitutive model has been established within the formalism of thermodynamics with internal variables and the most popular theories, namely, the von Mises, Tresca, Mohr–Coulomb and Drucker–Prager models, have been described in detail.

Obviously, due to the mathematical complexity of such constitutive theories, an exact solution to boundary value problems of practical engineering interest can only be obtained under very simplified conditions. The existing analytical solutions are normally restricted to perfectly plastic models and are used for the determination of limit loads and steady plastic flow of bodies with simple geometries (Chakrabarty, 1987; Hill, 1950; Lubliner, 1990; Prager, 1959; Skrzypek, 1993). The analysis of the behaviour of elastoplastic structures and soils under more realistic conditions requires the adoption of an adequate numerical framework capable of producing approximate solutions within reasonable accuracy. As pointed out in Chapter 4, the approximate solution to such problems is addressed in this book within the context of the Finite Element Method. In fact, the Finite Element Method is by far the most commonly adopted procedure for the solution of elastoplastic problems. Since the first reported applications of finite elements in plasticity in the mid-1960s, a substantial development of the related numerical techniques has occurred. Today, the Finite Element Method is regarded as the most powerful and reliable tool for the analysis of solid mechanics problems involving elastoplastic materials and is adopted by the vast majority of commercial software packages for elastoplastic stress analysis.

This chapter describes in detail the numerical/computational procedures necessary for the implicit finite element solution of small strain plasticity problems within the framework of Chapter 4. For the sake of generality, the methodologies presented in this chapter are initially derived taking the general plasticity model introduced in Chapter 6 (summarised in Box 6.2, page 151) as the underlying constitutive model. Practical application of the theory and procedures introduced, including a complete description of the algorithms and corresponding FORTRAN subroutines of the HYPLAS program, is then made to the particular case of the von Mises model with nonlinear isotropic hardening. The choice of this model is motivated here by the simplicity of its computational implementation. A set of numerical examples is also presented. Further application of the theory is made at the end of the chapter to a mixed isotropic/kinematic hardening version of the von Mises model. This model is also included in the HYPLAS program. Application to the Tresca, Mohr–Coulomb and Drucker–Prager models is left for Chapter 8.

Computational Methods for Plasticity: Theory and Applications EA de Souza Neto, D Perić and DRJ Owen